

A NOTE ON HOMOLOGICAL BERGLUND–HÜBSCH–HENNINGSON MIRROR SYMMETRY FOR CURVE SINGULARITIES

MATTHEW HABERMANN

ABSTRACT. In this note, we establish homological Berglund–Hübsch mirror symmetry for curve singularities where the A–model incorporates equivariance, otherwise known as homological Berglund–Hübsch–Henningson mirror symmetry. More precisely, we prove a conjecture of Futaki and Ueda [FU13, Conjecture 6.1] which posits that the equivariance in the A–model can be incorporated by pulling back the superpotential to the total space of the corresponding crepant resolution. Our approach is predicated on the fact that the Morsifications used in [HS20] are equivariant with respect to the group actions appearing on the A–side of the conjecture. Along the way, we show that the category of matrix factorisations of the mirror has a tilting object whose length is the dimension of the state space of the closed string FJRW A–model. The construction of this tilting object might also be of independent interest in algebraic geometry and representation theory, in that it partially extends [BIY20, Theorem 2.1] by allowing for more general grading groups.

1. INTRODUCTION

Given a polynomial $f : X \rightarrow \mathbb{C}$ with an isolated singularity at the origin, one can naturally associate two categories to it; one by studying the singularity defined by f symplectically (the A–model), and the other by studying it algebraically (the B–model). The first category is called the Fukaya–Seidel category of f , $\mathcal{FS}(f)$, and is a categorification of the space of vanishing cycles. On the algebro-geometric side, one can study the (dg)-category of matrix factorisations, denoted by $\text{mf}(X, f)$. In the case where f is equivariant with respect to the action of an abelian group G which contains \mathbb{C}^* , one can also study the G -equivariant matrix factorisations, which is denoted by $\text{mf}(X, G, f)$.

Whilst there is no general prediction about how the Fukaya–Seidel category and the category of matrix factorisations (equivariant or otherwise) of f should be related, homological mirror symmetry predicts that certain singularities should arise in pairs, and, crucially for us, this pairing of singularities should respect equivariant structures. The main result of this note confirms this prediction in the case of invertible curve singularities, where we incorporate equivariance into the A–model by following a suggestion of Futaki and Ueda in [FU13].

To define an invertible polynomial, consider an $n \times n$ matrix A , invertible over \mathbb{Q} , with non-negative integer entries a_{ij} . To such a matrix, one can associate a polynomial $\mathbf{w} \in \mathbb{C}[x_1, \dots, x_n]$

$$\mathbf{w} = \sum_{i=1}^n \prod_{j=1}^n x_j^{a_{ij}}. \tag{1}$$

In what follows, we will always have that \mathbf{w} is quasi-homogeneous, with weight system given by $(d_0, d_1, \dots, d_n; h)$, where

$$\mathbf{w}(t^{d_1}x_1, \dots, t^{d_n}x_n) = t^h \mathbf{w}(x_1, \dots, x_n)$$

for any $t \in \mathbb{C}^*$, and $d_0 := h - \sum_{i=1}^n d_i$. In [BH92], the authors define the transpose of \mathbf{w} by associating to A^T a polynomial $\check{\mathbf{w}}$ and a weight system $(\check{d}_0, \dots, \check{d}_n; \check{h})$; we call this the Berglund–Hübsch transpose. We call the polynomial \mathbf{w} *invertible* if it is of the form (1) for some A , it is quasi-homogeneous, and both \mathbf{w} and $\check{\mathbf{w}}$ define isolated singularities at the origin.

Recall that for $f \in \mathbb{C}[x_1, \dots, x_n]$ and $g \in \mathbb{C}[y_1, \dots, y_m]$, their Thom–Sebastiani sum is defined as

$$f \boxplus g = f \otimes 1 + 1 \otimes g \in \mathbb{C}[x_1, \dots, x_n, y_1, \dots, y_m]. \quad (2)$$

A corollary of Kreuzer–Skarke’s classification of quasi-homogeneous polynomials, [KS92], is that any invertible polynomial can be decoupled into the Thom–Sebastiani sum of *atomic* polynomials of the following three types:

- Fermat: $\mathbf{w} = x_1^{p_1}$,
- Loop: $\mathbf{w} = x_1^{p_1}x_2 + x_2^{p_2}x_3 + \dots + x_n^{p_n}x_1$,
- Chain: $\mathbf{w} = x_1^{p_1}x_2 + x_2^{p_2}x_3 + \dots + x_n^{p_n}$.

The Thom–Sebastiani sums of polynomials of Fermat type are also called Brieskorn–Pham.

Example 1.1. Consider the matrix $A = \begin{pmatrix} 3 & 0 & 0 \\ 1 & 3 & 0 \\ 0 & 0 & 2 \end{pmatrix}$. The corresponding polynomial is the E_7 singularity, and is the Thom–Sebastiani sum of $x^3 + xy^3$ and z^2 . In fact, ADE singularities in all dimensions are examples of invertible polynomials.

A key piece of data which is associated to an invertible polynomial \mathbf{w} is its *maximal symmetry group*

$$\Gamma_{\mathbf{w}} := \{(t_1, \dots, t_n, t_{n+1}) \in (\mathbb{C}^*)^{n+1} \mid t_1^{a_{1,1}} \dots t_n^{a_{1,n}} = \dots = t_1^{a_{n,1}} \dots t_n^{a_{n,n}} = t_{n+1}\}.$$

In other words, by setting $\chi_{\mathbf{w}}$ to be the character given by projection onto t_{n+1} , and where $\Gamma_{\mathbf{w}}$ acts on \mathbb{C}^n in the obvious way, \mathbf{w} is $\Gamma_{\mathbf{w}}$ -equivariant of degree $\chi_{\mathbf{w}}$. Note that t_{n+1} is completely determined by the other t_i , and so we consider $\Gamma_{\mathbf{w}} \subseteq (\mathbb{C}^*)^n$. Since \mathbf{w} is quasi-homogeneous, there is a natural inclusion

$$\begin{aligned} \varphi : \mathbb{C}^* &\rightarrow \Gamma_{\mathbf{w}} \\ t &\mapsto (t^{d_1}, \dots, t^{d_n}). \end{aligned}$$

We call any subgroup of finite index of $\Gamma_{\mathbf{w}}$ containing the image of φ *admissible*. The B–model of the homological mirror symmetry prediction we consider will be a pair (\mathbf{w}, Γ) , where Γ is an admissible subgroup. In the case where $\Gamma = \Gamma_{\mathbf{w}}$, we call \mathbf{w} (and the corresponding transpose $\check{\mathbf{w}}$) *maximally graded*, and drop $\Gamma_{\mathbf{w}}$ from the notation.

To translate Γ -equivariance to grading by an abelian group, we begin by encoding $\Gamma_{\mathbf{w}}$ -equivariance by the abelian group $L_{\mathbf{w}}$, which is freely generated by the elements $\vec{x}_1, \dots, \vec{x}_n$ (the degrees of x_1, \dots, x_n , respectively) and \vec{c} (the degree of \mathbf{w}) modulo the relations

$$\sum_{j=1} a_{ij} \vec{x}_j = \vec{c} \text{ for all } i.$$

The group L corresponding to equivariance by an admissible subgroup $\Gamma \subseteq \Gamma_{\mathbf{w}}$ is then a quotient of $L_{\mathbf{w}}$.

The case of homological mirror symmetry for maximally graded invertible polynomials has garnered a lot of attention; however, there has recently been much interest in the non-maximally graded case. To work in this setting, we need to introduce the notion of Berglund–Henningson dual group, defined as

$$\check{\Gamma} := \text{Hom}(\Gamma_{\mathbf{w}}/\Gamma, \mathbb{C}^*). \quad (3)$$

Note that, by construction, this is a subgroup of $\ker \chi_{\check{\mathbf{w}}} \subseteq \text{SL}(n, \mathbb{C})$, the group of symmetries with respect to which $\check{\mathbf{w}}$ is *invariant*. This generalisation of invertible polynomials to include different symmetry groups was initially studied in [BH95] and further explored in [Kra10]. By [ET12, Proposition 3], the definition given above of $\check{\Gamma}$ is a reformulation¹ of [Kra10, Definition 15].

¹Strictly speaking, the cited result pertains to the closely related maximal group of symmetries which keeps \mathbf{w} invariant, although the resulting quotient, and therefore dual groups, are the same.

Roughly speaking, homological Berglund–Hübsch–Henningson mirror symmetry predicts that (\mathbf{w}, Γ) and $(\check{\mathbf{w}}, \check{\Gamma})$ should be a mirror pair of (equivariant) singularities. More precisely:

Conjecture 1. *Let \mathbf{w} be an invertible polynomial with admissible group of symmetries Γ and $\check{\mathbf{w}}$ its Berglund–Hübsch transpose with dual grading group $\check{\Gamma}$. Then, there is a quasi-equivalence of \mathbb{Z} -graded pre-triangulated A_∞ -categories over \mathbb{C}*

$$\mathrm{mf}(\mathbb{C}^n, \Gamma, \mathbf{w}) \simeq \mathcal{FS}_{\check{\Gamma}}(\check{\mathbf{w}}).$$

In Conjecture 1, the category $\mathcal{FS}_{\check{\Gamma}}(\check{\mathbf{w}})$ is the $\check{\Gamma}$ -equivariant (or orbifold) Fukaya–Seidel category of $\check{\mathbf{w}}$. In the case $\Gamma = \Gamma_{\mathbf{w}}$, $\check{\Gamma} = 1$, and this reduces to the Fukaya–Seidel category of $\check{\mathbf{w}}$ defined in [Sei08]. In this case, the conjecture is known as homological Berglund–Hübsch mirror symmetry, and can be traced back to [Ued06] and [Tak10]. See also [LU22, Conjecture 1.2] and references therein. The conjecture has been established for Brieskorn–Pham polynomials and Thom–Sebastiani sums of singularities of type A and D in [FU11] and [FU13], respectively, as well as for all invertible curve singularities in [HS20]. Moreover, strong evidence for the conjecture in the case of chain polynomials was provided in [PV21], where it was shown that the B–model satisfies a certain recursion relation for directed A_∞ -categories, and details for the corresponding argument on the A–side where sketched in detail.

In general, the definition of an equivariant Fukaya–Seidel category is a difficult problem ([FU09, Problem 3]), even in the case of a Lefschetz fibration whose fibres are preserved by the group action, as studied in [CH17, Section 13.1]. On the other hand, if one begins with a hypersurface singularity, $\check{\mathbf{w}}$, one must, at least in the original formulation of [Sei08], Morsify $\check{\mathbf{w}}$ in order to construct the Fukaya–Seidel category. Whilst Morsifications abound, these will, in general in the case where $\check{\mathbf{w}}$ is equivariant with respect to a group action, not respect this equivariant structure. As an approach to defining an orbifold Fukaya–Seidel category which avoids the need to Morsify, Cho, Choa and Jeong construct a new $\mathbb{Z}/2$ -graded A_∞ -category which they take as the orbifold Fukaya–Seidel category and conjecture that it agrees with the standard definition in the non-equivariant case ([CCJ20, Conjecture 5.6]). Their definition stems from an understanding of the wrapped Fukaya category of the orbifold Milnor fibre, and is inspired by the classical variation operator ([CCJ20, Theorem 2.1]). With this definition, they prove the corresponding statement of Conjecture 1 in the $\mathbb{Z}/2$ -graded case of curves ([CCJ20, Theorem 1.3]).

Our approach is orthogonal to that of [CCJ20], where we observe that the *resonant Morsifications* introduced in [HS20] keep $\check{\mathbf{w}}$ invariant with respect to the action of $\check{\Gamma}$. We then exploit this fact to establish a version of Conjecture 1 proposed in [FU13], which we now explain.

The main result of this note concerns an approach in two variables suggested by Futaki and Ueda, where one replaces the category $\mathcal{FS}_{\check{\Gamma}}(\check{\mathbf{w}})$ with $\mathcal{FS}(\check{\mathbf{w}})$, which is defined as follows. Firstly, observe that $\check{\Gamma} \simeq \mu_\ell$ for $\ell = [\Gamma_{\mathbf{w}} : \Gamma]$ and that this group acts diagonally on \mathbb{C}^2 by $\xi \cdot (\check{x}, \check{y}) = (\xi \check{x}, \xi^{-1} \check{y})$. Since $\check{\Gamma} \subseteq \ker \chi_{\check{\mathbf{w}}}$, we have that $\check{\mathbf{w}}$ descends to a map

$$\check{\mathbf{w}} : X \rightarrow \mathbb{C},$$

where $X = \mathbb{C}^2/\mu_\ell$ is the $A_{\ell-1}$ singularity. Then, let

$$\pi : \tilde{X} \rightarrow X$$

be the crepant resolution of X and define

$$\check{\tilde{\mathbf{w}}} := \pi^* \check{\mathbf{w}} : \tilde{X} \rightarrow \mathbb{C}.$$

In the same way as the Fukaya–Seidel category of an isolated hypersurface singularity is defined to be the Fukaya–Seidel category of any Morsification, we define $\mathcal{FS}(\check{\mathbf{w}})$ to be the Fukaya–Seidel category associated to $\check{\tilde{\mathbf{w}}}_\varepsilon$, the pullback of an equivariant Morsification of $\check{\mathbf{w}}$. Note that it is important to equivariantly Morsify and then pull back, rather than pull back and then Morsify, since pulling

back $\check{\mathbf{w}}$ will, in general, yield a map which is singular along the entire exceptional locus. We will discuss the issue of symplectic form on \tilde{X} in Section 3.1, although note that \tilde{X} will no longer be exact since the curves comprising the exceptional divisor are holomorphic.

With notation as above, Futaki–Ueda make the following conjecture:

Conjecture 2 ([FU13, Conjecture 6.1]). *Let \mathbf{w} be an invertible polynomial in two variables with admissible group of symmetries Γ and $\check{\mathbf{w}}$ its Berglund–Hübsch transpose with dual grading group $\check{\Gamma}$. Then, there is a quasi-equivalence of \mathbb{Z} -graded pre-triangulated A_∞ -categories over \mathbb{C}*

$$\mathrm{mf}(\mathbb{C}^2, \Gamma, \mathbf{w}) \simeq \mathcal{FS}(\check{\mathbf{w}}).$$

Our main result establishes the following:

Theorem 1. *Conjecture 2 holds for all invertible curve singularities.*

Note that Theorem 1 is a \mathbb{Z} -graded quasi-equivalence, in contrast to [CCJ20, Theorem 1.3]. On the other hand, their strategy has the advantage of incorporating any subgroup of $\ker \chi_{\check{\mathbf{w}}}$ on the A-side, not just those corresponding to admissible subgroups of $\Gamma_{\mathbf{w}}$. Moreover, their definition of orbifold Fukaya–Seidel category is applicable in higher dimensions, whereas ours exploits several facts which are only true in this dimension. Nevertheless, working in the \mathbb{Z} -graded setting allows us to deduce a corollary which might be of independent interest in representation theory and algebraic geometry.

A famous result of Seidel [Sei08, Theorem 18.24] establishes that the Fukaya–Seidel category of a singularity has a full exceptional collection given by Lagrangian thimbles. Combining this with Conjecture 1 in the maximally graded case yields the prediction that $\mathrm{mf}(\mathbb{C}^n, \Gamma_{\mathbf{w}}, \mathbf{w})$ should have a full exceptional collection of length $\mu(\check{\mathbf{w}})$, the Milnor number of the *transpose polynomial*. Strengthening this, Lekili and Ueda conjectured that $\mathrm{mf}(\mathbb{C}^n, \Gamma_{\mathbf{w}}, \mathbf{w})$ should have a tilting object of length $\mu(\check{\mathbf{w}})$ ([LU22, Conjecture 1.3]). Slightly stronger still is the prediction of Hirano and Ouchi that this tilting object should come from a full and *strong* exceptional collection ([HO20, Conjecture 1.4]). This was shown for invertible polynomials in $n \leq 3$ variables in [Kra19] and for all chain polynomials in [HO20]. Moreover, it was established in [FKK20] that the category of matrix factorisations for any maximally graded invertible polynomial has a full exceptional collection of the predicted length, and that this collection is strong under an additional (and mild) Gorenstein hypothesis.

Importantly, Seidel’s result is formulated in the setting where the total space is exact and the Landau–Ginzburg model is not equivariant. Therefore, the evidence for predicting a full (strong) exceptional collection of a given length becomes weaker in the non-maximally graded setting. Nevertheless, the construction of a tilting object is a key element of our proof of Theorem 1, and we establish the following:

Corollary 1. *Let \mathbf{w} be an invertible polynomial in two variables with admissible group of symmetries Γ of index ℓ and $\check{\mathbf{w}}$ its Berglund–Hübsch transpose with dual grading group $\check{\Gamma}$. Then, $\mathrm{mf}(\mathbb{C}^2, \Gamma, \mathbf{w})$ has a tilting object of length*

$$\frac{\mu(\check{\mathbf{w}}) - 1}{\ell} + \ell.$$

The length of this tilting object can be seen as being predicted by closed-string mirror symmetry, where one studies the FJRW A–model [FJR13]. The state space of this theory is defined as

$$\mathcal{H}_{\check{\mathbf{w}}, \check{\Gamma}} := \bigoplus_{\gamma \in \check{\Gamma}} \mathcal{H}_\gamma^{\check{\Gamma}},$$

where $\mathcal{H}_\gamma = H^{\dim_{\mathbb{C}} S_\gamma}(\mathbb{C}^{\dim_{\mathbb{C}} S_\gamma}, \Lambda_\gamma; \mathbb{C})$ for $S_\gamma = \mathrm{Spec} \mathbb{C}[x_1, \dots, x_n]^\gamma$ the fixed locus of γ , $\check{\mathbf{w}}|_{S_\gamma}$ is the restriction of $\check{\mathbf{w}}$ to this fixed locus, and Λ_γ is the stop in S_γ determined by $\check{\mathbf{w}}|_{S_\gamma}$. In the case that $\check{\Gamma} = 1$, this is just the space of Lefschetz thimbles and its dimension is $\mu(\check{\mathbf{w}})$. Given that

the Fukaya–Seidel category is a categorification of this space, one might optimistically suggest that $\mathcal{FS}_{\check{\Gamma}}(\check{\mathbf{w}})$ should categorify $\mathcal{H}_{\check{\mathbf{w}}, \check{\Gamma}}$ and have a full exceptional collection whose length is the dimension of the FJRW state space. If this were true, Conjecture 1 would then imply that $\text{mf}(\mathbb{C}^n, \Gamma, \mathbf{w})$ has a full exceptional collection of length $\dim_{\mathbb{C}} \mathcal{H}_{\check{\mathbf{w}}, \check{\Gamma}}$, and the desideratum would be that this collection is in fact strong, implying the existence of a tilting object. Whilst this is a long chain of hypothetical implications, Corollary 1 directly confirms this in the case of curves. In general, this might be too much to hope for, although establishing under which conditions such a tilting object exists would be interesting in its own right.

As already mentioned, Corollary 1 relates to previous work at the intersection of algebraic geometry and representation theory independently of homological mirror symmetry. Namely, with the exception of $x^2 + y^2$, all invertible polynomials in two variables yield L -graded Gorenstein rings of Krull dimension one with *negative* Gorenstein parameter. The existence of a tilting object for \mathbb{Z} -graded Gorenstein rings of Krull dimension one with non-positive Gorenstein parameter was established in [BIY20, Theorem 1.2], and our corollary can be seen as a partial generalisation of [BIY20, Theorem 2.1], which specifically studies \mathbb{Z} -graded hypersurface singularities $\mathbf{k}[x, y]/(f)$ where $|x| = |y| = 1$. In *loc. cit.*, \mathbf{k} is any field, although our result is only proven over \mathbb{C} .

1.1. Strategy of proof. Broadly speaking, our strategy of proof follows that of [HS20]. Namely, we begin by studying the category $\text{mf}(\mathbb{C}^2, \Gamma, \mathbf{w})$, showing that it has a tilting object, which we call \mathcal{E} . In order to study the A–model, a key element of our proof is the fact that the resonant Morsifications which were utilised in *loc. cit.* are in fact $\check{\Gamma}$ -invariant, meaning that it descends to X and can then be pulled back to \tilde{X} , resulting in the map $\check{\tilde{\mathbf{w}}}_\varepsilon : \tilde{X} \rightarrow X$ which has Morse critical points, and whose smooth fibre is the quotient of the Milnor fibre of $\check{\mathbf{w}}$ by $\check{\Gamma}$. With this set-up, our approach reduces to the familiar strategy, albeit in the non-exact setting. Namely, we describe the directed category $\mathcal{A}_{\check{\Gamma}}$ associated to vanishing cycles in the smooth fibre of $\check{\tilde{\mathbf{w}}}_\varepsilon$. We then establish mirror symmetry by showing that, at the level of cohomology, $\mathcal{A}_{\check{\Gamma}}$ matches the endomorphism algebra of \mathcal{E} before appealing to formality to establish the corresponding chain-level statement.

1.2. Structure of the paper. As in [HS20], we begin by considering the loop case, first studying the B–model in Section 2 and the A–model in Section 3. We then consider the chain case in Sections 4 and 5, and Brieskorn–Pham polynomials in Section 6, although it should be emphasised that all technical details, both in general and as they differ from the maximally graded case are already present in the loop case; the chain and Brieskorn–Pham cases are essentially simplifications.

1.3. Acknowledgements. The author would like to thank Jack Smith for his collaboration in [HS20], of which this work is an outgrowth, and also for valuable comments on an earlier draft of this note. The author gratefully acknowledges support from the University of Hamburg and the Deutsche Forschungsgemeinschaft under Germany’s Excellence Strategy – EXC 2121 “Quantum Universe” – 390833306.

2. LOOP B-MODEL

In this section, our main goal is to study the dg-category of Γ -equivariant matrix factorisations, $\text{mf}(\mathbb{C}^2, \Gamma, \mathbf{w})$, where $\mathbf{w} = x^p y + y^q x$ and $\Gamma \subseteq \Gamma_{\mathbf{w}}$ is an admissible subgroup of the maximal grading group of index $\ell \leq d = \gcd(p-1, q-1)$. Without loss of generality, we will assume $p \geq q \geq 2$. As in the maximally graded case, we will encode this equivariance by an L -grading, where L is a rank one abelian group with cyclic torsion.

Recall that $L_{\mathbf{w}}$ is generated by \vec{x} , \vec{y} and \vec{c} , modulo the relations

$$p\vec{x} + \vec{y} = \vec{x} + q\vec{y} = \vec{c},$$

which is equivalent to the group \mathbb{Z}^2 quotiented by the subgroup generated by $(p-1, 1-q)$. Correspondingly, for $\Gamma \subseteq \Gamma_{\mathbf{w}}$ of index ℓ ,

$$L \simeq \mathbb{Z}^2 / \left(\frac{p-1}{\ell}, \frac{1-q}{\ell} \right) \simeq \mathbb{Z} \oplus \mathbb{Z} / \left(\frac{d}{\ell} \right).$$

We will consider this as the group generated by \vec{x} and \vec{y} modulo the relation $\frac{p-1}{\ell} \vec{x} = \frac{q-1}{\ell} \vec{y}$, and note that $L/\mathbb{Z}\vec{c} \simeq \mathbb{Z}/\left(\frac{pq-1}{\ell}\right)$. Consider $S = \mathbb{C}[x, y]$ as an L -graded ring with $|x| = \vec{x}$ and $|y| = \vec{y}$ such that \mathbf{w} is a quasi-homogeneous polynomial of degree \vec{c} . Furthermore, we write $R = S/(\mathbf{w})$; note that this notation is consistent with Futaki–Ueda [FU13], but opposite to that of Dyckerhoff [Dyc11]. It is straightforward to calculate that this is an L -graded Gorenstein ring with Gorenstein parameter² $\alpha = \vec{x} + \vec{y} - \vec{c}$. Recall that graded Gorenstein means that there is an isomorphism

$$\mathrm{RHom}_{\mathrm{gr}-R}(\mathbb{C}, R(-\alpha)) \simeq \mathbb{C}[-n],$$

where α is the Gorenstein parameter, n is the Krull dimension of R , and $M(l)$ for an L -graded R (or S) module is an internal grading shift such that $M(l)_i = M_{i+l}$. The Gorenstein parameter α is *negative* (resp. zero, positive) if its projection to the \mathbb{Z} -factor of L is negative (resp. zero, positive). For an invertible polynomial, this value is $-d_0$, which is negative for all invertible polynomials other than $x^2 + y^2$, where it is zero.

Later, we will utilise Serre duality for maximal Cohen–Macaulay (MCM) modules which follows from Auslander–Reiten duality ([AR87]). Recall that an R -module is MCM if $\mathrm{Ext}_{\mathrm{gr}-R}^i(M, R) = 0$ for all $i > 0$, and the *stabilised* category of maximal Cohen–Macaulay modules, denoted by MCM(R), has the same objects as MCM(R), but the morphisms are given by

$$\underline{\mathrm{Hom}}_{\mathrm{gr}-R}(M, N) := \mathrm{Hom}_{\mathrm{gr}-R}(M, N)/\mathcal{P}(M, N),$$

where $\mathcal{P}(M, N)$ are those morphisms which factor through a projective R -module. For any $M, N \in \mathrm{MCM}(R)$ such that $\mathrm{Hom}_{\mathrm{gr}-R}(M, N)$ is finite dimensional there is then Serre duality

$$\underline{\mathrm{Hom}}_{\mathrm{gr}-R}(M, N) \simeq \underline{\mathrm{Hom}}_{\mathrm{gr}-R}(N, M(-\alpha)[n-1])^\vee, \quad (4)$$

where $(-)^{\vee}$ is the \mathbb{C} -linear dual and n is again the Krull dimension of R . Note that, in our case, the fact that \mathbf{w} has an *isolated* singularity means that all Hom-spaces are finite dimensional. For a proof of Serre duality in the \mathbb{Z} -grading case, we refer to [IT13, Corollary 3.5]; the L -graded case is a straightforward generalisation.

By an L -graded matrix factorisation of rank r , K^\bullet , we will mean a two periodic sequence of L -graded, rank r , S -modules

$$K^\bullet = (\cdots \rightarrow K^i \xrightarrow{k^i} K^{i+1} \xrightarrow{k^{i+1}} K^{i+2} \rightarrow \cdots),$$

where $k^{i+1} \circ k^i = \mathbf{w} \cdot \mathrm{Id}_r$, and graded two-periodicity means $K^\bullet(\vec{c}) \simeq K^\bullet[2]$. This presentation of a matrix factorisation naturally arises from the process of *stabilisation*; see, for example, [Dyc11, Sections 2.1 and 2.2]. Namely, one starts with a finitely generated R -module M , and considers an R -free resolution. By a famous result of Eisenbud ([Eis80]), any such resolution eventually becomes two periodic (i.e. stabilises). To get a matrix factorisation, we extend this two periodic complex indefinitely to the right and then replace the R modules in the complex by the corresponding S modules. The inverse of this process is given by taking the cokernel of the map k^0 . In fact, there is an equivalence of categories

$$\mathrm{coker} : \mathrm{HMF}(\mathbb{C}^2, \Gamma, \mathbf{w}) \xrightarrow{\sim} \underline{\mathrm{MCM}}(R),$$

where $\mathrm{HMF}(\mathbb{C}^2, \Gamma, \mathbf{w})$ is the homotopy category of $\mathrm{mf}(\mathbb{C}^2, \Gamma, \mathbf{w})$.

A different perspective on the category of matrix factorisations is provided by a famous result of

²It is also common, for example in [IT13], to refer to the a -invariant of R , which is the negative of the Gorenstein parameter.

Buchweitz and Orlov ([Buc86], [Orl09, Theorem 39]), which, generalised to stacks in [PV11] and applied to our setting, shows that

$$D_{\text{sg}}^b([\mathbf{w}^{-1}(0)/\Gamma]) \simeq \text{HMF}(\mathbb{C}^2, \Gamma, \mathbf{w}).$$

In the above, the category on the left is the derived category of singularities of the stack $[\mathbf{w}^{-1}(0)/\Gamma]$, which is defined as the quotient of the derived category of coherent sheaves on $[\mathbf{w}^{-1}(0)/\Gamma]$ by the subcategory of perfect complexes. Moreover, L -graded R -modules naturally correspond to sheaves on $[\mathbf{w}^{-1}(0)/\Gamma]$, yielding an equivalence

$$D_{\text{sg}}^b(\text{gr } R) \simeq D_{\text{sg}}^b([\mathbf{w}^{-1}(0)/\Gamma]).$$

Justified by the above equivalences, we will frequently switch between talking about graded R -modules, sheaves on $[\mathbf{w}^{-1}(0)/\Gamma]$ and matrix factorisations. Moreover, observe that (4) and these equivalences gives Serre functors on each of the categories we consider.

In order to study the basic objects, we introduce the notation $\mathbf{w} = xyw_1 \dots w_\ell$, where

$$w_r = x^{\frac{p-1}{\ell}} - e^{\frac{\pi\sqrt{-1}}{\ell}} \eta^r y^{\frac{q-1}{\ell}}$$

for η a primitive ℓ^{th} root of unity. Continuing with notation introduced in [HS20, Section 2.2], we define $w = w_1 \dots w_\ell$. With this, there are $\ell + 2$ matrix factorisations coming from (Γ -equivariantly) factoring \mathbf{w} . These correspond to

$$\begin{aligned} K_x^\bullet &= (\dots \rightarrow S(-\vec{c}) \xrightarrow{yw} S(-\vec{x}) \xrightarrow{x} S \rightarrow \dots), \\ K_y^\bullet &= (\dots \rightarrow S(-\vec{c}) \xrightarrow{xw} S(-\vec{y}) \xrightarrow{y} S \rightarrow \dots), \end{aligned}$$

as well as the matrix factorisations

$$K_{w_r}^\bullet = (\dots \rightarrow S(-\vec{c}) \xrightarrow{\mathbf{w}/w_r} S(-\frac{p-1}{\ell}\vec{x}) \xrightarrow{w_r} S \rightarrow \dots).$$

These matrix factorisations are the obvious generalisation of the maximally graded case, and, as in this case, we also consider the objects

$$\begin{aligned} {}^i K_x &= K_x((i+1-p)\vec{x}) \\ {}^j K_y &= K_y((i+1-q)\vec{y}) \end{aligned}$$

where $i = p - \frac{p-1}{\ell}, \dots, p-1$ and $j = q - \frac{q-1}{\ell}, \dots, q-1$.

On the other hand, the generalisation of the matrix factorisations corresponding to sheaves supported at the origin require more technical considerations. Namely, for $p - \frac{p-1}{\ell} \leq i \leq p-1$, $1 \leq j \leq q-1$, we set $k = \lfloor \frac{(j-1)\ell}{q-1} \rfloor$ and consider the ideal

$$I_{i,j} = (x^{i-(\ell-1-k)\frac{p-1}{\ell}}, x^{i-(\ell-k)\frac{p-1}{\ell}} y^{j-k\frac{q-1}{\ell}}, \dots, x^{i-(\ell-1)\frac{p-1}{\ell}} y^{j-\frac{q-1}{\ell}}, y^j)$$

and the L -graded R -modules

$$R((i+1)\vec{x} + (j+1)\vec{y})/I_{i,j}.$$

Remark 2.1. It might seem objectionable that the symmetry which exists between p and q has been broken in the above ideals; however, we will later see that, for example, taking the ideals corresponding to $1 \leq i \leq p-1$ and $q - \frac{q-1}{\ell} \leq j \leq q-1$, would lead to a tilting object whose endomorphism algebra corresponds to the same quiver-with-relations as the choice we have made – cf. Remark 2.8.

The corresponding matrix factorisation, which we denote by ${}^{i,j} K_0$, is given by stabilising this module. In particular, an R -free resolution can be built by beginning with

$$R(\vec{c} - (k+1)\frac{p-1}{\ell}\vec{x} + j\vec{y}) \oplus \bigoplus_{t=0}^{k-1} R(\vec{c}) \oplus R((i+1)\vec{x} + \vec{y}) \xrightarrow{(x^{i-(\ell-1-k)\frac{p-1}{\ell}} \dots y^j)} R((i+1)\vec{x} + (j+1)\vec{y}),$$

yielding a rank $(k + 2)$ matrix factorisation.

From this, it is straightforward to check that maps defining the matrix factorisation are given in even degree by

$$d_0 = \begin{pmatrix} y^{j-k} \frac{q-1}{\ell} & 0 & 0 & \dots & 0 & x^{p-i+\frac{p-1}{\ell}(\ell-1-k)} y \\ -x^{\frac{p-1}{\ell}} & y^{\frac{q-1}{\ell}} & 0 & \dots & 0 & 0 \\ 0 & -x^{\frac{p-1}{\ell}} & y^{\frac{q-1}{\ell}} & \dots & 0 & 0 \\ 0 & 0 & -x^{\frac{p-1}{\ell}} & \dots & 0 & 0 \\ \vdots & \vdots & \vdots & \ddots & \vdots & \vdots \\ 0 & 0 & 0 & \dots & y^{\frac{q-1}{\ell}} & 0 \\ 0 & 0 & 0 & \dots & -x^{i-(\ell-1)\frac{p-1}{\ell}} & xy^{q-j} \end{pmatrix}, \quad (5)$$

and in odd degree by $d_1 = \text{Adj}(d_0)$, the adjugate matrix. Explicitly, we have that ${}^{i,j}K_0$ corresponds to the matrix factorisation

$$\begin{array}{ccc} S(\vec{c} - \frac{p-1}{\ell}\vec{x}) & S(\vec{c} - (k+1)\frac{p-1}{\ell}\vec{x} + j\vec{y}) & S(2\vec{c} - \frac{p-1}{\ell}\vec{x}) \\ \oplus & \oplus & \oplus \\ \cdots \oplus_{t=0}^{k-1} S(\vec{c} - \frac{p-1}{\ell}\vec{x}) & \xrightarrow{d_0} \oplus_{t=0}^{k-1} S(\vec{c}) & \xrightarrow{d_1} \oplus_{t=0}^{k-1} S(2\vec{c} - \frac{p-1}{\ell}\vec{x}) \cdots \\ \oplus & \oplus & \\ S((i+1)\vec{x} + (j+1)\vec{y} - \vec{c}) & S((i+1)\vec{x} + \vec{y}) & S((i+1)\vec{x} + (j+1)\vec{y}) \end{array}$$

where the rightmost term is in cohomological degree 0.

As in the maximally graded case, we are interested in a full subcategory \mathcal{B} of $\text{mf}(\mathbb{A}^2, \Gamma, \mathbf{w})$ consisting of the objects described above. Namely, let \mathcal{B} be the category consisting of the $\frac{pq-1}{\ell} + \ell$ objects

$$\{{}^{i,j}K_0, {}^iK_x[3], {}^{q-\frac{q-1}{\ell}}K_y[3], \dots, {}^{q-1}K_y[3], K_{w_1}[3], \dots, K_{w_\ell}[3]\}_{i=p-\frac{p-1}{\ell}, \dots, p-1; j=1, \dots, q-1}.$$

The reason for the shifts is so that all morphisms turn out to have cohomological degree 0. In the following sections we compute the morphisms between the objects in this category. The reader willing to take these computations on faith may skip directly to Theorem 2.7 for the characterisation of \mathcal{B} as a quiver algebra.

2.1. Morphisms between the K_x 's, K_y 's and K_{w_r} 's. As before, we leverage a result of Buchweitz [Buc86, Section 1.3, Remark (a)] which claims the following: given L -graded R -modules M and M' with corresponding stabilisations K and K' , we have

$$\text{Hom}_{\text{HMF}(\mathbb{C}^2, \Gamma, \mathbf{w})}^\bullet(K, K') \simeq H^\bullet(\text{Hom}_{\text{gr}-R}(K \otimes_S R, M'))$$

The Hom on the right-hand side is taken component-wise on the complex $K \otimes_S R$. Note that this requires that the ring be Gorenstein, as proven in [Kra19, Proposition 2.23], where we also refer to for proof of the statement.

Remark 2.2. Strictly speaking, Buchweitz's result only applies for $\bullet \gg 0$; however, since $[2] \simeq (\vec{c})$ in $\text{HMF}(\mathbb{C}^2, \Gamma, \mathbf{w})$, we can always achieve that the degree is high enough for the theorem to apply, and this does not affect the result of the calculation.

For calculations regarding the modules K_x , K_y and K_{w_r} , the arguments carry over almost verbatim from the maximally graded case [HS20, Sections 2.3 and 2.4], and we have:

Lemma 2.3. *In $\text{HMF}(\mathbb{C}^2, \Gamma, \mathbf{w})$, we have the following:*

- (i) *For any $i \in \mathbb{Z}$, the objects ${}^iK_x, \dots, {}^{i+\frac{p-1}{\ell}-1}K_x$ are exceptional and pairwise orthogonal.*
- (ii) *For any $j \in \mathbb{Z}$, the objects ${}^jK_y, \dots, {}^{j+\frac{q-1}{\ell}-1}K_y$ are exceptional and pairwise orthogonal.*

- (iii) The objects $K_{w_1}, \dots, K_{w_\ell}$ are exceptional pairwise orthogonal
- (iv) For each $i = p - \frac{p-1}{\ell}, \dots, p-1$, $j = q - \frac{q-1}{\ell}, \dots, q-1$, $r = 1, \dots, \ell$, ${}^i K_x$, ${}^j K_y$ and K_{w_r} are mutually orthogonal. \square

2.2. Morphisms between the K_{w_r} 's and K_0 's. The fact that $\text{Hom}^\bullet(K_{w_r}, {}^{i,j}K_0) = 0$ essentially follows from the arguments of [HS20, Section 2.5]. In the other direction $\text{Hom}^\bullet({}^{i,j}K_0, K_{w_r})$ we argue as follows. Firstly, observe that, since \mathbf{w} has an isolated singularity at the origin, morphisms of R -modules are finite dimensional, and Serre duality for the corresponding CM modules applies. We then observe that

$$\dim_{\mathbb{C}} \text{Hom}^\bullet(K_{w_r}, {}^{i,j}K_0(\vec{c} - \vec{x} - \vec{y})) = \begin{cases} 1 & \text{if } \bullet = -3 \\ 0 & \text{otherwise,} \end{cases} \quad (6)$$

and so $\text{Hom}^\bullet({}^{i,j}K_0, K_{w_r})$ is non-trivial only in cohomological degree three, where it is rank one; it is then straightforward to write down this non-trivial element.

Lemma 2.4. *For each $r = 1, \dots, \ell$, there is a single morphism between ${}^{i,j}K_0$ and K_{w_r} given by*

$$\text{Hom}^3({}^{i,j}K_0, K_{w_r}) = \mathbb{C} \cdot \begin{pmatrix} y^{(k+1)\frac{q-1}{\ell} - j} \\ e^{-\frac{\pi i}{\ell}} \eta^{-r} \\ (e^{-\frac{\pi i}{\ell}} \eta^{-r})^2 \\ \vdots \\ (e^{-\frac{\pi i}{\ell}} \eta^{-r})^k \\ (e^{-\frac{\pi i}{\ell}} \eta^{-r})^{k+1} x^{p-1-i} \end{pmatrix}.$$

Proof. Observe that the complex computing the morphisms has differential given by d_0^T in odd degree and $d_1^T = \text{Adj}(d_0)^T$ in even degree, where d_0 is the map from (5). It is then clear that the above vector defines an element in the kernel; the only non-trivial term to check is that it is in the kernel of the last row of d_0^T , although this follows from observing that this factors into $(\ell - 1 - k)$ polynomials, one of which is w_r . It is clear that this is not in the image of d_1^T , since the $k - 1$ constant elements in the kernel cannot be in the image of a degree $\frac{p-1}{\ell} \vec{x}$ -map. The fact that this spans the cohomology group follows from (6). \square

2.3. Morphisms between K_x 's and K_y 's and K_0 's. For each I we have that $\text{Hom}^\bullet({}^I K_x, {}^{i,j}K_0)$ vanishes, which can be computed in the same way as in the maximally graded case. In order to compute the morphisms in the other direction, we argue again by Serre duality. In particular, we have that

$$\dim_{\mathbb{C}} \text{Hom}^\bullet({}^I K_x, {}^{i,j}K_0(\vec{c} - \vec{x} - \vec{y})) = \begin{cases} 1 & \text{if } I = i, \bullet = -3 \\ 0 & \text{otherwise,} \end{cases} \quad (7)$$

and similarly there is only one morphism $\text{Hom}^\bullet({}^J K_x, {}^{i,j}K_0(\vec{c} - \vec{x} - \vec{y}))$ in degree negative three when $J \equiv j \pmod{\frac{q-1}{\ell}}$, and is zero otherwise. Note that the complexes computing cohomology do not vanish identically in the cases where we claim the cohomology is zero, as in Section 2.2, but the complexes are exact.

Lemma 2.5. *In $\text{HMF}(\mathbb{C}^2, \Gamma, \mathbf{w})$ there are no morphisms from ${}^I K_x$ to ${}^{i,j}K_0$. There are no morphisms in the other direction unless $I = i$, in which case the morphism space is spanned by $(0, 0, \dots, 0, 1)$ in degree 3. Similarly, the only morphisms between ${}^J K_y$ and ${}^{i,j}K_0$ are from the latter to the former, and are given by $(1, 0, \dots, 0)$ in degree 3 when $j \equiv J \pmod{\frac{q-1}{\ell}}$.*

Proof. The proof follows the same strategy as the proof of Lemma 2.4. Namely, the statement about the morphisms between ${}^I K_x$ and ${}^{i,j}K_0$ is immediate after observing that multiplication by y^\bullet is exact, and the only morphism from ${}^{i,j}K_0$ to ${}^I K_x$ is in degree three. The statement about morphisms between ${}^J K_y$ and ${}^{i,j}K_0$ is proved similarly, although this time multiplication by x^\bullet is exact. \square

2.4. Morphisms between K_0 's. Computing morphisms ${}^{i,j}K_0 \rightarrow {}^{I,J}K_0$ is analogous to the maximally graded case. Namely, morphisms are spanned by the module

$$(R/I_{I,J})_{(I-i)\vec{x} + (J-j)\vec{y}}.$$

From this, it is immediate that there are no morphisms unless $J \geq j$; however, unlike in the maximally graded case, it is now possible to have $i > I$ since $\frac{p-1}{\ell}\vec{x} = \frac{q-1}{\ell}\vec{y}$. Putting this together, we conclude:

Lemma 2.6. *For all $i \in \{p - \frac{p-1}{\ell}, \dots, p-1\}$ and $j \in \{1, \dots, q-1\}$, we have*

$$\text{Hom}^\bullet({}^{i,j}K_0, {}^{I,J}K_0) \simeq \begin{cases} \text{span}\{x^{I-i}y^{J-j}, \dots, x^{I-i+k\frac{p-1}{\ell}}y^{(J-j) \bmod \frac{q-1}{\ell}}\} & \text{if } I \geq i, J \geq j \\ & \text{and } \bullet = 0 \\ \text{span}\{x^{I-i+\frac{p-1}{\ell}}y^{J-j-\frac{q-1}{\ell}}, \dots, x^{I-i+k\frac{p-1}{\ell}}y^{(J-j) \bmod \frac{q-1}{\ell}}\} & \text{if } I < i, \\ & J \geq j + \frac{q-1}{\ell} \\ & \text{and } \bullet = 0 \\ 0 & \text{otherwise.} \end{cases} \quad \square$$

2.5. The total endomorphism algebra of the basic objects. From the results of the previous sections, we see that the objects in \mathcal{B} are all exceptional. In fact, the endomorphism algebra of the objects in \mathcal{B} are presented as a quiver-with-relations:

Theorem 2.7. *The cohomology-level total endomorphism algebra of the objects of \mathcal{B} is the algebra of the quiver-with-relations described in Figure 1, with all arrows living in degree zero. In particular, \mathcal{B} is a \mathbb{Z} -graded A_∞ -category concentrated in degree 0, so is intrinsically formal.*

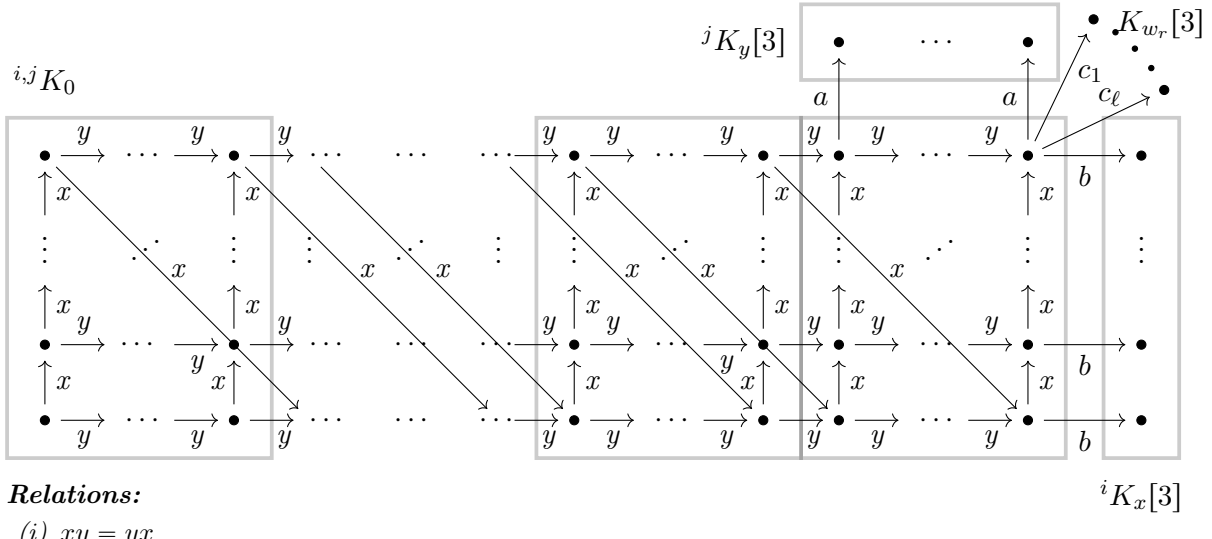


FIGURE 1. The quiver describing the category \mathcal{B} for loop polynomials.

Proof. In order to prove the statement, all that is required is to show that the morphisms of matrix factorisations above compose in the way corresponding to the relations of the quiver. The first and second relations follow from the maximally graded case *mutatis mutandis*, although the third relation is not present in the maximally graded case. Without loss of generality, it suffices to prove

the relation where

$$x^{\frac{p-1}{\ell}}, y^{\frac{q-1}{\ell}} \in \text{Hom}^0(p-1, (\ell-1) \frac{q-1}{\ell} K_0, p-1, q-1 K_0),$$

$$c_r \in \text{Hom}^3(p-1, q-1 K_0, K_{w_r}).$$

In odd degrees, the morphism of matrix factorisations corresponding to $x^{\frac{p-1}{\ell}}$ is given by the $(\ell+1) \times \ell$ matrix

$$\begin{pmatrix} 1 & 0 & 0 & \dots & 0 \\ 0 & 1 & 0 & \dots & 0 \\ 0 & 0 & 1 & \dots & 0 \\ \vdots & \vdots & \vdots & \ddots & \vdots \\ 0 & 0 & 0 & \dots & 1 \\ 0 & 0 & 0 & \dots & 0 \end{pmatrix},$$

and similarly the morphism $y^{\frac{q-1}{\ell}}$ is given in odd degrees by the matrix of the same form as above with a row of zeros in the first row and then the $\ell \times \ell$ identity matrix underneath. It is then straightforward to check that the third relation holds. \square

Remark 2.8. Following on from Remark 2.1, it is here that it becomes evident that the resulting category is independent of the choice of representatives for ${}^{i,j}K_0$. In particular, making different choices would lead to rearranging the blocks in Figure 1, which is evidently the same quiver. For example if one were to choose ${}^{i,j}K_0$ with $i = 1, \dots, p-1$ and $j = q - \frac{q-1}{\ell}, \dots, q-1$ with $I_{i,j}$ changed appropriately, the resulting quiver would have the blocks drawn vertically and the relations would be the same.

Example 2.9. Consider the polynomial $x^p y + y^p x$ with $\ell = p-1$. Then, the corresponding quiver is given by

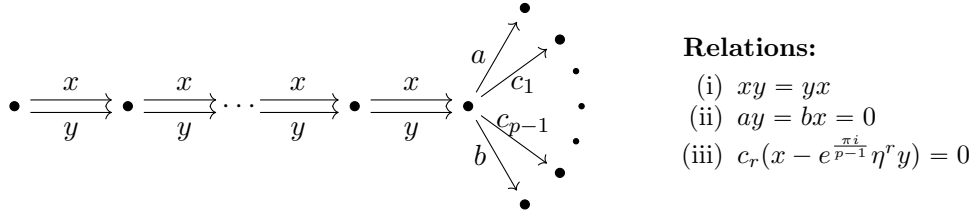


FIGURE 2. Quiver corresponding to $x^p y + y^p x$.

This corresponds to a tilting object of the \mathbb{Z} -graded ring $\mathbb{C}[x, y]/(x^p y + y^p x)$ with $|x| = |y| = 1$, and is a special case of [BIY20, Theorem 2.1].

2.6. Generation. Now that we have characterised the full subcategory $\mathcal{B} \subseteq \text{HMF}(\mathbb{A}^2, \Gamma, \mathbf{w})$, we aim to show that it generates. To this end, we utilise the following result of Polishchuk-Vaintrob:

Lemma 2.10 ([PV16, Proposition 2.3.1], cf. [Dyc11, Corollary 5.3]). *The category $\text{HMF}(\mathbb{C}^2, \Gamma, \mathbf{w})$ is split-generated by the L-grading shifts of the stabilisation of the module $R/(x, y)$. \square*

After showing that $\text{HMF}(\mathbb{A}^2, \Gamma, \mathbf{w})$ is split-generated by \mathcal{B} , we then appeal to the facts that \mathcal{B} is intrinsically formal and $\text{Tw } \mathcal{B}$ is idempotent complete to prove:

Proposition 2.11. *The functor*

$$\text{Tw } \mathcal{B} \rightarrow \text{mf}(\mathbb{C}^2, \Gamma, \mathbf{w})$$

is a quasi-equivalence.

Proof. Our proof is broadly similar to the maximally graded case of [HS20, Proposition 2.14], with only minor modifications needed to incorporate the change of grading. Namely, let

$$V = \{{}^i K_x, {}^j K_y, K_{w_r}, {}^{i,j} K_0\}$$

be the objects of \mathcal{B} . We then show that $R(l)/(x, y) \in \langle V \rangle$ for any $l \in L$ and appeal to Lemma 2.10 to show that V split-generates $\text{HMF}(\mathbb{C}^2, \Gamma, \mathbf{w})$. Since \mathcal{B} is intrinsically formal, it also split generates $\text{mf}(\mathbb{C}^2, \Gamma, \mathbf{w})$, i.e., there is a quasi-equivalence

$$\text{Tw}^\pi \mathcal{B} \rightarrow \text{mf}(\mathbb{C}^2, \Gamma, \mathbf{w}).$$

To show *generation*, observe that, since \mathcal{B} is a full exceptional collection in $\text{Tw } \mathcal{B}$, the latter is already idempotent complete, as explained in [Sei08, Remark 5.14]. Therefore, taking the idempotent completion of $\text{Tw } \mathcal{B}$ does nothing, and we get the result.

Since [2] is equivalent to (\vec{c}) , we must only show that $R(l)/(x, y) \in \langle V \rangle$ for $l \in L/\mathbb{Z}\vec{c} \simeq \mathbb{Z}/\left(\frac{pq-1}{\ell}\right)$. The argument to build the modules

$$\begin{aligned} & \{R(a\vec{x} + b\vec{y})/(x, y)\}_{\{p - \frac{p-1}{\ell} + 1 \leq a \leq p, 2 \leq b \leq q\}} \\ & \{R(a\vec{x} + \vec{y})/(x, y)\}_{\{p - \frac{p-1}{\ell} \leq a \leq p-1\}} \\ & \{R((p - \frac{p-1}{\ell})\vec{x} + b\vec{y})/(x, y)\}_{\{1 \leq b \leq \frac{q-1}{\ell} + 1\}} \end{aligned}$$

with the exception of $R((p - \frac{p-1}{\ell})\vec{x} + \vec{y})/(x, y)$ in the second collection of modules and $R(\vec{c})/(x, y)$ in the third carry over from [HS20, Proposition 2.14] essentially unchanged. Note that, along the way, we built the modules $R(a\vec{x})/(x), R(b\vec{y})/(y) \in \langle V \rangle$ for $1 \leq a \leq p-1$ and $b = 1, \dots, q-1$.

To build $R((p - \frac{p-1}{\ell})\vec{x} + \vec{y})/(x, y)$, observe that $K_{w_1}[1] = R((p - \frac{p-1}{\ell})\vec{x} + \vec{y})/(xyw_2 \dots w_\ell)$, and that there is a morphism

$$R(\frac{p-1}{\ell}\vec{x})/(w_2) \xrightarrow{xyw_3 \dots w_\ell} R((p - \frac{p-1}{\ell})\vec{x} + \vec{y})/(xyw_2 \dots w_\ell),$$

whose cone is $R((p - \frac{p-1}{\ell})\vec{x} + \vec{y})/(xyw_3 \dots w_\ell)$. The codomain is $K_{w_1}[1]$, whilst the domain is the module $K_{w_r}(\frac{p-1}{\ell}\vec{x})$ for $r = 2$, and is built as follows. We begin by observing that

$$R(\vec{x})/(w_r) \simeq \text{Cone}\left(R((1 - \frac{p-1}{\ell})\vec{x})/(x) \xrightarrow{w_r} R(\vec{x})/(xw_r)\right).$$

The domain of this morphism is ${}^{p-\frac{p-1}{\ell}} K_x$, whilst the codomain can be constructed as an extension of $R(\vec{x})/(x)$ by $R/(w_r)$. We then proceed inductively to construct $K_{w_r}(l\vec{x})$ for $l = 0, \dots, (\ell-1)\frac{p-1}{\ell}$. With these modules constructed, we then iteratively take cones of morphisms

$$R((r-1)\frac{p-1}{\ell}\vec{x})/(w_r) \xrightarrow{xyw_{r+1} \dots w_\ell} R((p - \frac{p-1}{\ell})\vec{x} + \vec{y})/(xyw_r \dots w_\ell),$$

until we are left with $R((p - \frac{p-1}{\ell})\vec{x} + \vec{y})/(xy)$. We then construct $R((p - \frac{p-1}{\ell})\vec{x} + \vec{y})/(x, y)$ as the cone of the morphism

$$\begin{aligned} & R((\ell-1)\frac{p-1}{\ell}\vec{x} + \vec{y})/(y) \\ & \oplus \quad \xrightarrow{(x \ y)} \quad R((p - \frac{p-1}{\ell})\vec{x} + \vec{y})/(xy) \\ & R((p - \frac{p-1}{\ell})\vec{x})/(x) \end{aligned}$$

Finally, the module $R/(x, y)$ is constructed analogously to $R((p - \frac{p-1}{\ell})\vec{x} + \vec{y})/(x, y)$ as a cone, where the domain is the direct sum of $R(-\vec{x})/(y)$ and $R(-\vec{y})/(x)$, and the codomain is $R/(xy)$. Firstly, we build $R((p-2)\vec{x})/(w_1 \dots w_\ell)[-2]$ as the cone of $R((q-1)\vec{y}) \xrightarrow{w_1 \dots w_\ell} R((2q-1)\vec{y})/(yw_1 \dots w_\ell)$, where the codomain is $R((p-1)\vec{x})/(x)[1]$. Then, $R(-\vec{x})/(y)$ is the extension of $R((p-1)\vec{x})/(x)$ by

$R((p-2)\vec{x})/(w_1 \dots w_\ell)$. The module $R/(xy) \simeq R((q-1)\vec{y})/(w_1 \dots w_\ell)$, on the other hand, is built from $R(q\vec{y})/(y) \simeq R(-\vec{x})/(y)[2]$ and $R(q\vec{y})/(yw_1 \dots w_\ell) \simeq R/(x)[1]$. \square

We deduce the following corollary, whose proof follows from Proposition 2.11 and Theorem 2.7 in the same way as in the proof of [HS20, Theorem 2.19]:

Corollary 2.12 (Corollary 1, loop polynomial case). *The object*

$$\mathcal{E} := \left(\bigoplus_{\substack{i=p-\frac{p-1}{\ell}, \dots, p-1 \\ j=1, \dots, q-1}} {}^i {}^j K_0 \right) \oplus \left(\bigoplus_{i=p-\frac{p-1}{\ell}, \dots, p-1} {}^i K_x[3] \right) \oplus \left(\bigoplus_{j=q-\frac{q-1}{\ell}, \dots, q-1} {}^j K_y[3] \right) \oplus \left(\bigoplus_{r=1, \dots, \ell} K_{w_r}[3] \right)$$

is a tilting object for $\mathrm{mf}(\mathbb{C}^2, \Gamma, \mathbf{w})$.

3. LOOP A-MODEL

3.1. The crepant resolution of the $A_{\ell-1}$ singularity. We begin this section with a recounting of the classically understood crepant³ resolution of du Val singularities of type A – see, for example [Rei03]. This subsection will be applicable to all invertible polynomials in two variables.

Recall that the $A_{\ell-1}$ singularity is defined as $\mathbb{C}^2/\mu_\ell = X = \mathrm{Spec} \mathbb{C}[u, v, w]/(uv - w^\ell)$, where μ_ℓ acts by $\xi \cdot (\check{x}, \check{y}) = (\xi \check{x}, \xi^{-1} \check{y})$. The crepant resolution is

$$\pi : \tilde{X} \rightarrow X,$$

where

$$\tilde{X} = \bigcup_{i=1}^{\ell} \tilde{X}_i,$$

and each $\tilde{X}_i \simeq \mathbb{C}_{(\lambda_i, \mu_i)}^2$, for $\lambda_i = u/w^{i-1}$, $\mu_i = w^i/u$ and transition functions

$$\begin{aligned} \tilde{X}_i \setminus (\mu_i = 0) &\xrightarrow{\sim} \tilde{X}_{i+1} \setminus (\lambda_{i+1} = 0) \\ (\lambda_i, \mu_i) &\mapsto (\mu_i^{-1}, \mu_i^2 \lambda_i). \end{aligned}$$

On each chart, the resolution is given as

$$\begin{aligned} \pi|_{\tilde{X}_i} : \mathbb{C}_{(\lambda_i, \mu_i)}^2 &\rightarrow X \\ (\lambda_i, \mu_i) &\mapsto (\lambda_i^i \mu_i^{i-1}, \lambda_i^{\ell-i} \mu_i^{\ell+1-i}, \lambda_i \mu_i). \end{aligned}$$

An important point is which symplectic form one puts on the total space \tilde{X} . Of course, this is diffeomorphic to the Milnor fibre of the $A_{\ell-1}$ singularity, although choosing the associated symplectic form would have the wrong properties. In particular, the rational curves in the exceptional locus would be Lagrangian spheres, as opposed to holomorphic. As such, observe that \tilde{X} cannot be exact as a symplectic manifold.

In order to define the symplectic form we consider, observe that there is a natural inclusion of \tilde{X} into the product of \mathbb{C}^3 with $\lfloor \frac{\ell}{2} \rfloor$ copies of \mathbb{P}^2 given by the blowing up process. We define the symplectic form $\omega_{\tilde{X}}$ to be the pullback of the product of the standard symplectic form on \mathbb{C}^3 and the Fubini–Study form on the \mathbb{P}^2 factors. We also drop \tilde{X} from the notation and refer to the symplectic form simply as ω , since we believe that no confusion can arise. This form is simple to write down in a

³Recall that a resolution $\pi : \tilde{X} \rightarrow X$ is *crepant* if $\pi^* K_X \simeq K_{\tilde{X}}$.

given patch, although has quite a few terms. As an example, in the patch \tilde{X}_1 , it is given by

$$\begin{aligned} \phi_1^*\omega = \frac{i}{2} & \left((1 + |\mu_1|^2 + |\mu_1|^4) d\lambda_1 \wedge d\bar{\lambda}_1 + (\lambda_1 \bar{\mu}_1 + 2|\mu_1|^2 \lambda_1 \bar{\mu}_1) d\mu_1 \wedge d\bar{\mu}_1 \right. \\ & + (\mu_1 \bar{\lambda}_1 + 2|\mu_1|^2 \mu_1 \bar{\lambda}_1) d\lambda_1 \wedge d\bar{\mu}_1 + (4|\lambda_1|^2 |\mu_1|^2 + |\lambda_1|^2) d\mu_1 \wedge d\bar{\mu}_1 \\ & \left. + \frac{(1 + 4|\mu_1|^2 + |\mu_1|^4) d\mu_1 \wedge d\bar{\mu}_1}{(1 + |\mu_1|^2 + |\mu_1|^4)^2} \right), \end{aligned}$$

where $\phi_1 : \tilde{X}_1 \rightarrow \tilde{X}$ is the inclusion of the chart $\tilde{X}_1 \simeq \mathbb{C}^2$.

Finally, we note that, whilst the A–model strategy follows that of [HS20], there are technical subtleties in this setting due to the non-exactness. In particular, the exactness of the total space is key in the construction of the Fukaya–Seidel category in [Sei08] by ruling out sphere and disc bubbling. Since our total space is non-exact, we follow the strategy of [AKO08, Section 3], who also allow for non-exact total spaces and Lagrangians by demanding the following two conditions:

- (i) The smooth fibre Σ is exact,
- (ii) The homotopy group $\pi_2(\Sigma)$ and the relative homotopy group $\pi_2(\Sigma, V_i)$, for any (potentially non-exact) vanishing cycle V_i , vanish.

These conditions are both fulfilled in our case, and thus the construction of the Fukaya–Seidel category is well defined. As in *loc. cit.*, we take $\text{Tw } \mathcal{A}_{\tilde{\Gamma}}$ as the definition of this category.

3.2. A resonant Morsification. In the maximally graded case studied in [HS20, Section 3], a Morsification $\tilde{\mathbf{w}}_\varepsilon = \tilde{x}^p \tilde{y} + \tilde{y}^q \tilde{x} - \varepsilon \tilde{x} \tilde{y}$ with particularly nice properties was used. Such a Morsification was called *resonant*, and allowed the symmetry present to be maintained and ultimately exploited. Whilst it was not considered in the maximally graded setting, the resonant Morsifications are in fact also *equivariant* for any $\tilde{\Gamma} \simeq \mu_\ell$. Therefore, such a Morsification descends to a map $\tilde{\mathbf{w}}_\varepsilon : X \rightarrow \mathbb{C}$ given by

$$\tilde{\mathbf{w}}_\varepsilon(u, v, w) = w(u^{\frac{p-1}{\ell}} + v^{\frac{q-1}{\ell}} - \varepsilon).$$

Pulling this back to the chart $\tilde{X}_i \simeq \mathbb{C}_{(\lambda_i, \mu_i)}^2$ of the crepant resolution \tilde{X} yields

$$\tilde{\mathbf{w}}_{i,\varepsilon}(\lambda_i, \mu_i) = \lambda_i \mu_i \left(\lambda_i^{\frac{i(p-1)}{\ell}} \mu_i^{\frac{(i-1)(p-1)}{\ell}} + \lambda_i^{\frac{(\ell-i)(q-1)}{\ell}} \mu_i^{\frac{(\ell+1-i)(q-1)}{\ell}} - \varepsilon \right),$$

and this patches together to give a globally defined map $\tilde{\mathbf{w}}_\varepsilon : \tilde{X} \rightarrow \mathbb{C}$. Note that, like invertible polynomials, the maps $\tilde{\mathbf{w}}_{i,\varepsilon}$ are all *tame at infinity* in the sense of [Bro88, Definition 3.1]. This follows directly from [Bro88, Proposition 3.1]. From now on, we will refer to the restrictions of $\tilde{\mathbf{w}}_\varepsilon$ to the charts as $\tilde{\mathbf{w}}_i$, with the reference to ε left implicit.

Analogously to the maximally graded case, the critical points of $\tilde{\mathbf{w}}_\varepsilon$ can be grouped into four types:

- (i) $\mu_1 = 0, \lambda_1^{\frac{p-1}{\ell}} = \varepsilon$
- (ii) $\mu_\ell^{\frac{q-1}{\ell}} = \varepsilon, \lambda_\ell = 0$
- (iii) $\mu_i = \lambda_i = 0$ for $i = 1, \dots, \ell$
- (iv) $\lambda_1^{\frac{p-1}{\ell}} = \frac{q-1}{pq-1} \varepsilon, \lambda_1^{\frac{(\ell-1)(q-1)}{\ell}} \mu_1^{q-1} = \frac{p-1}{pq-1} \varepsilon$.

Note that the critical points of type (iv) can equivalently be described in any of the charts of \tilde{X} ; we have given them in the first for convenience. The first three critical points have critical value 0, whilst the last has critical value

$$\frac{-\varepsilon \mu_1 \lambda_1}{pq-1}.$$

As in our previous work, there is a clear symmetry of these critical points. Namely, let $(\lambda_{1,\text{crit}}^+, \mu_{1,\text{crit}}^+)$ be the unique positive real critical point of type (iv) in the chart \tilde{X}_1 , with corresponding critical value c_{crit} . Letting ζ and η denote the roots of unity

$$\zeta = e^{2\pi i/(p-1)} \quad \text{and} \quad \eta = e^{2\pi i/(q-1)}, \quad (8)$$

we see that there is a $\mu_{p-1} \times \mu_{q-1}$ action on the critical points of type (iv) given by

$$\{(\zeta^{m\ell} \lambda_{1,\text{crit}}^+, \zeta^{m(1-\ell)} \eta^n \mu_{1,\text{crit}}^+) : 0 \leq m \leq p-2, 0 \leq n \leq q-2\}.$$

The critical value corresponding to $(\zeta^{m\ell} \lambda_{1,\text{crit}}^+, \zeta^{m(1-\ell)} \eta^n \mu_{1,\text{crit}}^+)$ is $\zeta^m \eta^n c_{\text{crit}}$, so there are $\frac{\gcd(p-1, q-1)}{\ell}$ critical points in each of these critical fibres. We therefore restrict to the subset

$$\{(\zeta^{m\ell} \lambda_{1,\text{crit}}^+, \zeta^{m(1-\ell)} \eta^n \mu_{1,\text{crit}}^+) : 0 \leq m \leq \frac{p-1}{\ell} - 1, 0 \leq n \leq q-2\}$$

to describe all of the critical points of type (iv).

Remark 3.1. Whilst it appears that we are making a choice in the above, we will see later that choosing different elements of $\mu_{p-1} \times \mu_{q-1}$ leads to on-the-nose the same result, as in Remark 2.8 on the B-side. The reason is that choosing a different subset of $\mu_{p-1} \times \mu_{q-1}$ corresponds to the same critical points, but the vanishing paths we will shortly describe will be different.

Our strategy for understanding the Fukaya–Seidel category of $\tilde{\mathbf{w}}_\varepsilon$ is essentially modelled on the strategy of the maximally graded case. Namely, we fix our regular fibre Σ to be $\tilde{\mathbf{w}}_1^{-1}(-\delta)$ where δ is a positive real number much less than ε (in other words, we take $* = -\delta$). This reference fibre is equivalently described in any of the charts, and is equivalent, since each $\tilde{\mathbf{w}}_i$ is tame, to the quotient of the Milnor fibre of $\tilde{\mathbf{w}}$ by $\tilde{\Gamma}$, as studied in [Hab21, Section 7.1.1]. For the critical points of types (i)–(iii) we follow the strategy we employed in the maximally graded case and define the vanishing path given by the straight line segment from $-\delta$ to 0. For the critical point $(\zeta^{m\ell} \lambda_{1,\text{crit}}^+, \zeta^{m(1-\ell)} \eta^n \mu_{1,\text{crit}}^+)$, meanwhile, we define the *preliminary vanishing path* $\gamma_{m,n}$ by following the circular arc $-\delta e^{i\theta}$ as θ increases from 0 to

$$\theta_{m,n} := 2\pi \left(\frac{m}{p-1} + \frac{n}{q-1} \right)$$

and then following the radial straight line segment from $-\zeta^m \eta^n \delta$ to $\zeta^m \eta^n c_{\text{crit}}$. The preliminary vanishing paths are then altered to the temporary, and then final, vanishing paths in the same way as the maximally graded case.

3.3. The zero-fibre and its smoothing. The fibre of $\tilde{\mathbf{w}}_\varepsilon$ over zero has $\ell + 2$ components: in the charts \tilde{X}_1 and \tilde{X}_ℓ , there are the line $\{\mu_1 = 0\}$ and $\{\lambda_\ell = 0\}$, respectively. The planes $(0, \mu_i)$ and $(\lambda_{i+1}, 0)$ patch together to give $\ell - 1$ projective lines in an $A_{\ell-1}$ configuration. Finally, there is the curve given in local charts by $\check{w}_i = \tilde{\mathbf{w}}_i \lambda_i^{-1} \mu_i^{-1}$. This fibre is sketched in Figure 3.

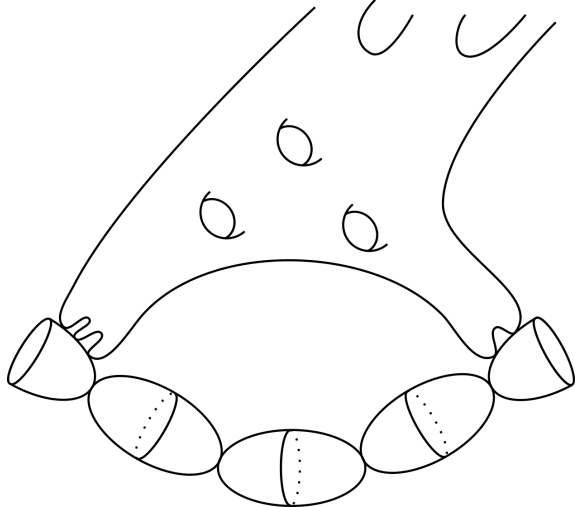


FIGURE 3. Sketch of the fibre of \check{w}_ε above the origin.

Upon smoothing, each of the nodes is smoothed to a thin neck whose waist curve is the corresponding vanishing cycle in Σ . We denote these vanishing cycles by ${}^m V_{\mu_1 \check{w}_1}$, ${}^n V_{\lambda_\ell \check{w}_\ell}$ and $V_{\mu_i \lambda_i}$ for $m = 0, \dots, \frac{p-1}{\ell} - 1$, $n = 0, \dots, \frac{q-1}{\ell} - 1$ and $i = 1, \dots, \ell$, corresponding to critical points $(\zeta^{m\ell} \varepsilon^{\ell/(p-1)}, 0)$, $(0, \eta^{n\ell} \varepsilon^{\ell/(q-1)})$ and $(\lambda_i, \mu_i) = (0, 0)$ respectively⁴.

Remark 3.2. The topology of the smooth fibre was computed in [Hab21, Section 7.1.1]. Namely, it is a curve of genus

$$g(\Sigma) = \frac{1}{2\ell}(pq - 1 - \gcd(\ell(p-1), p+q-2))$$

with

$$2 + \gcd(p-1, \frac{p+q-2}{\ell})$$

boundary punctures. Note that this could also have been deduced in the same way as in [HS20, Remark 3.1], although, since the $V_{\mu_i \lambda_i}$ are homologous, the rank of $H_1(\Sigma; \mathbb{Z})$ is $\frac{pq-1}{\ell} + 1$, rather than the full $\frac{pq-1}{\ell} + \ell$.

As in our previous work, we argue that the monodromy of parallel transport around an arc of small enough radius δ is supported in the neck regions which emerge upon smoothing, and is the product of Dehn twists in these regions. After deleting these regions of Σ to obtain Σ' , we may trivialise the fibration \check{w}_ε over the disc of radius δ such the smooth fibre is given by Σ' . Concretely, Σ' comprises: the λ_1 -axis with small discs removed around the $\frac{p-1}{\ell}$ -th roots of ε , as well at the origin, the charts $\tilde{X}_i \simeq \mathbb{C}_{(\lambda_i, \mu_i)}^2$ for $i = 2, \dots, \ell - 1$ with a small disc around the origin removed, the μ_ℓ -axis with small discs around the $\frac{q-1}{\ell}$ -th roots of ε removed, as well as a disc around the origin in this chart, and lastly a $\frac{(p-1)(q-1)}{\ell}$ -fold cover of the line $\{u+v=\varepsilon\}$ with small discs around $(\varepsilon, 0)$ and $(0, \varepsilon)$ removed. Here, the covering map is given in the chart \tilde{X}_ℓ by $(\lambda_i, \mu_i) \mapsto (\lambda_i^{\frac{i(p-1)}{\ell}}, \mu_i^{\frac{(i-1)(p-1)}{\ell}}, \lambda_i^{\frac{(\ell-i)(q-1)}{\ell}}, \mu_i^{\frac{(\ell+1-i)(q-1)}{\ell}})$, although it is most convenient to consider it in the first or last charts, where the fact that it is a $\frac{(p-1)(q-1)}{\ell}$ -fold cover becomes obvious.

3.4. The preliminary vanishing cycles. Let ${}^{m,n}V_0^{\text{pr}}$ denote the preliminary vanishing cycle in Σ corresponding to the critical point $(\zeta^{m\ell} \lambda_{1,\text{crit}}^+, \zeta^{m(1-\ell)} \eta^n \mu_{1,\text{crit}}^+)$ and the preliminary vanishing path $\gamma_{m,n}$. In this subsection we explain the necessary alterations to the arguments in the maximally

⁴The symmetry of the critical points of type (ii) must be computed in the chart \tilde{X}_ℓ , which is the action given above under the change of coordinates.

graded case required in order to describe these cycles.

Since $\tilde{\mathbf{w}}_\varepsilon$ has real coefficients in a given chart, we can temporarily view it here as a map $\mathbb{R}^2 \rightarrow \mathbb{R}$. In the chart \tilde{X}_1 , this function has a local minimum at $(\lambda_{1,\text{crit}}^+, \mu_{1,\text{crit}}^+)$, where it attains the value $c_{\text{crit}} < 0$. There are no critical values in the interval $(c_{\text{crit}}, 0)$, so the level sets $\tilde{\mathbf{w}}_1^{-1}(c)$ for c in this range have a component which is a smooth loop encircling $(\lambda_{1,\text{crit}}^+, \mu_{1,\text{crit}}^+)$, and which shrinks down to this point as $c \searrow c_{\text{crit}}$. As $c \nearrow 0$ this loop, which we denote by Λ_c , converges to a piecewise smooth curve, Λ_0 , which is given in the chart \tilde{X}_i by the curves $\mu_i = 0$, $\lambda_i = 0$ and $\tilde{w}_i = \varepsilon$. It is worth reiterating that the curve \tilde{w} only intersects the coordinate planes of a given chart in the fibre over the origin only in \tilde{X}_1 and \tilde{X}_ℓ , where it intersects $\mu_1 = 0$ and $\lambda_\ell = 0$, respectively.

Returning to the full complex picture, we exploit the symmetry of the situation, as well as the fact that the monodromy of parallel transport around a small arc centred at the origin is supported in the discs which are removed to give Σ' . In particular, our main task is to understand the monodromy in these regions. Fortunately, since we have assumed ε to be sufficiently small, the symplectic form reduces to

$$\frac{i}{2}(d\lambda_i \wedge d\bar{\lambda}_i + d\mu_i \wedge d\bar{\mu}_i)$$

in the neck regions, meaning that only a minor adaptation of the parallel transport arguments of the maximally graded case is required. Namely, over a path $c(t)$ contained in a neck region where the symplectic form is as above, symplectic parallel transport between the fibres of $\tilde{\mathbf{w}}_\varepsilon$ is described by the ODE

$$\begin{pmatrix} \dot{\lambda}_i \\ \dot{\mu}_i \end{pmatrix} = \frac{\dot{c}}{|d\tilde{\mathbf{w}}_i|^2} \begin{pmatrix} \overline{\partial_{\lambda_i} \tilde{\mathbf{w}}_i} \\ \overline{\partial_{\mu_i} \tilde{\mathbf{w}}_i} \end{pmatrix}. \quad (9)$$

This equation clearly preserves the real part of the equation along the path which follows the negative real axis. Therefore, the loops Λ_c are taken to each other by parallel transport, and the loop $\Lambda_{-\delta}$ is the preliminary vanishing cycle ${}^{0,0}V_0^{\text{pr}}$.

Since the real preliminary vanishing cycle passes through each of the neck regions, the above argument is inherently global; however, we are able to use the local description of the symplectic form in each neck region and patch the result together since parallel transport only affects the part of the curve which passes through the neck region. In particular, how the curve is identified between patches is unaffected by parallel transport, since this happens away from the neck regions. Moreover, away from the neck regions, the curve ${}^{0,0}V_0^{\text{pr}}$ is particularly simple to describe: in the λ_1 -axis of \tilde{X}_1 , it comprises the real line segment joining the deleted ball at the origin to the deleted ball about the real $\frac{p-1}{\ell}$ -th root of ε , and in the μ_1 -projection, it is the straight line emanating from the deleted disc at the origin and going to infinity along the positive real axis. In both the λ_i and μ_i projections in the charts \tilde{X}_i for $i = 2, \dots, \ell - 1$, as well as the λ_ℓ projection in \tilde{X}_ℓ , it is similarly the straight line emanating from the deleted disc at the origin and going to infinity along the positive real axis. In the μ_ℓ -projection in the chart \tilde{X}_ℓ it is the straight line segment joining the deleted disc at the origin to the real $\frac{q-1}{\ell}$ -th root of ε in the μ_ℓ -plane. Finally, the rest of the curve is the positive real lift of the line segment joining the deleted balls about $(\varepsilon, 0)$ and $(0, \varepsilon)$ in $\{u + v = \varepsilon\}$ under the covering map described above. It is straightforward to check that, in each of the neck regions, the curve ${}^{0,0}V_0^{\text{pr}}$ is given by a hyperbola. For example, at the origin in the chart \tilde{X}_1 , it is given by

$$(\lambda_1, \mu_1) = \sqrt{\delta/\varepsilon}(e^s, e^{-s}) \quad (10)$$

where s is a small real variable.

Now that we understand the real vanishing cycle ${}^{0,0}V_0^{\text{pr}}$, we utilise the symmetry present in the situation to characterise ${}^{m,n}V_0^{\text{pr}}$. As before, we decompose $\gamma_{m,n}$ into its radial segment from $-\zeta^m \eta^n \delta$

to $\zeta^m \eta^n c_{\text{crit}}$ and circular segment from $-\delta$ to $-\zeta^m \eta^n \delta$. By construction, the map

$$\begin{aligned} f_{m,n}^{(i)} : \tilde{X}_i &\rightarrow \tilde{X}_i \\ (\lambda_i, \mu_i) &\mapsto (\zeta^{m(\ell+1-i)} \eta^{n(1-i)} \lambda_i, \zeta^{m(i-\ell)} \eta^{in} \mu_i) \end{aligned}$$

is a symplectomorphism on each patch with intertwines the transition map and fits together to yield a globally defined symplectomorphism $f_{m,n} : \tilde{X} \rightarrow \tilde{X}$ which intertwines the map $\tilde{\mathbf{w}}_\varepsilon : \tilde{X} \rightarrow \mathbb{C}$. It is therefore clear that $f_{m,n}(0,0 V_0^{\text{pr}})$ is the vanishing cycle corresponding to the straight line segment from $-\zeta^m \eta^n \delta$ to the critical point⁵ $(\zeta^{m\ell} \lambda_{1,\text{crit}}^+, \zeta^{m(1-\ell)} \eta^n \mu_{1,\text{crit}}^+)$, and a full description of ${}^{m,n}V_0^{\text{pr}}$ results from parallel transporting this around the arc from $-\zeta^m \eta^n \delta$ to $-\delta$. Since the monodromy of parallel transport along such an arc is contained in the neck regions, it is immediate that ${}^{m,n}V_0^{\text{pr}} = f_{m,n}(0,0 V_0^{\text{pr}})$ in Σ' , where it comprises: the straight line segment in the λ_1 -plane from the deleted disc about the origin to the deleted disc about the critical point $\zeta^{m\ell} \varepsilon^{\frac{p-1}{\ell}}$ (where $\varepsilon^{\frac{p-1}{\ell}}$ is the real root) and the straight line segment emanating from the deleted disc at the origin with argument $2\pi(\frac{m(1-\ell)}{p-1} + \frac{n}{q-1})$. Similarly, in the λ_i and μ_i projections in the chart \tilde{X}_i , the Lagrangian is given by the straight line segment emanating from the deleted disc at the origin with arguments $2\pi(\frac{m(\ell+1-i)}{p-1} + \frac{n(1-i)}{q-1})$ and $2\pi(\frac{m(i-\ell)}{p-1} + \frac{in}{q-1})$, respectively. In the λ_ℓ projection in the chart \tilde{X}_ℓ , the Lagrangian is emanating from the deleted disc at the origin with argument $2\pi(\frac{m}{p-1} + \frac{n(1-\ell)}{q-1})$, and in the μ_ℓ projection it is given by the straight line segment joining the deleted disc about the origin to the deleted disc about $\eta^{n\ell} \varepsilon^{\frac{q-1}{\ell}}$. Finally, the rest of the curve in Σ' is given by the lift of the line segment joining the deleted balls about $(\varepsilon, 0)$ and $(0, \varepsilon)$ in $\{u+v=\varepsilon\}$ to the $\zeta^{m\ell} \mathbb{R}_+ \times \zeta^{m(1-\ell)} \eta^n \mathbb{R}_+$ -locus in $\mathbb{C}^2 \simeq \tilde{X}_1$ under the projection described above. In the neck regions of Σ , the curve $f_{m,n}(0,0 V_0^{\text{pr}})$ is given by a parabola of the form (10), and to complete the description of ${}^{m,n}V_0^{\text{pr}}$, we must analyse how this changes under parallel transport along the arc from $-\zeta^m \eta^n \delta$ to $-\delta$ through the angle $\theta_{m,n}$.

In the neck region about the origin in a given chart, the polynomial $\tilde{\mathbf{w}}_i$ can be approximated by $-\varepsilon \lambda_i \mu_i$. Here, the parallel transport equation (9) becomes

$$\begin{pmatrix} \dot{\lambda}_i \\ \dot{\mu}_i \end{pmatrix} = \frac{-\dot{c}}{\varepsilon(|\lambda_i|^2 + |\mu_i|^2)} \begin{pmatrix} \bar{\mu}_i \\ \bar{\lambda}_i \end{pmatrix}. \quad (11)$$

Moreover, the $\zeta^{m(\ell+1-i)} \eta^{n(1-i)} \mathbb{R}_+ \times \zeta^{m(i-\ell)} \eta^{in} \mathbb{R}_+$ -locus in the $V_{\lambda_i \mu_i}$ -neck region is approximated by

$$(\lambda_i, \mu_i) = \sqrt{\delta/\varepsilon} (\zeta^{m(\ell+1-i)} \eta^{n(1-i)} e^s, \zeta^{m(i-\ell)} \eta^{in} e^{-s}).$$

Studying the solution to parallel transport over the line $c(t) = -\delta e^{it}$ as t ranges from $\theta_{m,n}$ to 0, we postulate a solution of the form $(\lambda_i, \mu_i) = \sqrt{\delta/\varepsilon} (e^{s+i\varphi}, e^{-s+i(t-\varphi)})$, where φ is a real function of s and t . Plugging this into (11) yields

$$\begin{pmatrix} \dot{\varphi} \lambda_i \\ (1 - \dot{\varphi}) \mu_i \end{pmatrix} = \frac{\lambda_i \mu_i}{|\lambda_i|^2 + |\mu_i|^2} \begin{pmatrix} \bar{\mu}_i \\ \bar{\lambda}_i \end{pmatrix}.$$

The initial condition is given by

$$\varphi(s, \theta_{m,n}) = 2\pi \left(\frac{m(\ell+1-i)}{p-1} + \frac{n(1-i)}{q-1} \right),$$

and so the general solution is calculated to be

$$\varphi(s, t) = 2\pi \left(\frac{m(\ell+1-i)}{p-1} + \frac{n(1-i)}{q-1} \right) + \frac{e^{-2s}(t - \theta_{m,n})}{e^{2s} + e^{-2s}}.$$

⁵We are free to describe the critical points of type (iv) in any chart, so we choose the first chart for simplicity.

in particular, the value of the function at the end of the parallel transport is given by

$$\begin{aligned}\varphi(s, 0) &= 2\pi \left(\frac{m(\ell+1-i)}{p-1} + \frac{n(1-i)}{q-1} \right) + \frac{-e^{-2s}\theta_{m,n}}{e^{2s} + e^{-2s}} \\ &= \frac{2\pi}{e^{2s} + e^{-2s}} \left(\frac{m(\ell+1-i)e^{2s} + m(\ell-i)e^{-2s}}{p-1} + \frac{n(1-i)e^{2s} - ine^{-2s}}{q-1} \right).\end{aligned}$$

This describes the argument of the λ_i -component of ${}^{m,n}V_0^{\text{pr}}$ (or the negative of the μ_i -component), and is in agreement with our expectation: as $s \rightarrow \infty$ this neck region joins the λ_i -axis, where we know that the λ_i -component of ${}^{m,n}V_0^{\text{pr}}$ has argument $2\pi \left(\frac{m(\ell+1-i)}{p-1} + \frac{n(1-i)}{q-1} \right)$. Similarly, as $s \rightarrow -\infty$, this neck region joins the μ_i -axis, where we know that the negative of the μ_i -component of ${}^{m,n}V_0^{\text{pr}}$ has argument $2\pi \left(\frac{m(\ell-i)}{p-1} - \frac{in}{q-1} \right)$. Note that $\arg \lambda_1 = \arg \lambda_2 = \dots = \arg \lambda_\ell$, and similarly for the arguments of μ_i . We therefore see that, if we view the smooth fibre as being glued from cylinders as in [Hab22, Section 3.2] and coordinatise the middle cylinder as upwards⁶ being in the positive λ_i direction, that the Lagrangian ${}^{m,n}V_0$ enters the middle cylinder with λ_ℓ argument $-\frac{2\pi\ell n}{q-1}$ from the left (which we are thinking of as being the ℓ^{th} neck region), and winds upwards – increasing the argument of λ_i – by $\frac{2\pi\ell m}{p-1} + \frac{2\pi\ell n}{q-1}$ degrees to exit the right hand side of the cylinder (the first neck region) at $\frac{2\pi\ell m}{p-1}$ degrees, as in Figure 4.

In order to fully describe the curve ${}^{m,n}V_0^{\text{pr}}$ in the smooth fibre, we run analogous arguments about the other neck regions in which the Lagrangian passes – namely, the balls deleted about the point $\zeta^{m\ell}\varepsilon^{\frac{1}{p-1}}$ on the λ_1 -axes and the point $\eta^{n\ell}\varepsilon^{\frac{q-1}{p-1}}$ on the μ_ℓ -axis. In the neck region corresponding to ${}^mV_{\mu_1\check{w}_1}$ we run the same argument as above, but this time with local coordinate λ'_1 , where $\lambda_1 = \zeta^{m\ell}\lambda_{1,\text{crit}}^+ - \lambda'_1$, and in this case it is the coordinate λ'_1 which interpolates from $\frac{2\pi\ell m}{p-1}$ to $2\pi \left(\frac{m(\ell-1)}{p-1} - \frac{in}{q-1} \right)$. The analogous statement is true about the neck corresponding to ${}^nV_{\lambda_\ell\check{w}_\ell}$. Moreover, the $\{\check{w}_i = \varepsilon\}$ part of the curve is essentially uninteresting, since the corresponding components of the different ${}^{m,n}V_0^{\text{pr}}$ in this segment are different lifts of the same segment in $\{u+v=\varepsilon\}$.

Remark 3.3. From the above description, it is clear that the analogue of [HS20, Remark 3.2] holds. Namely, for two Lagrangians ${}^{m,n}V_0$ and ${}^{M,N}V_0$ with $0 < m-M < \frac{p-1}{\ell}$ and $\kappa \frac{q-1}{\ell} < n-N < (\kappa+1) \frac{q-1}{\ell}$, the difference in λ_i arguments varies monotonically from $-2\pi(n-N)\ell/(q-1)$ to $2\pi(m-M)\ell/(p-1)$. The second term is strictly positive, and the first satisfies $2\pi(\kappa+1) < -2\pi(n-N)\ell/(q-1) < -2\pi\kappa$, so the arguments of these two curves are equal modulo 2π precisely $\kappa+1$ times. In addition, they intersect transversally at each of these points. Similarly, when $0 < M-m < \frac{p-1}{\ell}$ and $\kappa \frac{q-1}{\ell} < n-N < (\kappa+1) \frac{q-1}{\ell}$ for $\kappa \geq 1$, there are precisely κ transverse intersection, in clear analogy with the B-model.

3.5. Modifying the vanishing paths. As in [HS20, Section 3.4], the vanishing paths constructed above do not form a distinguished basis; indeed, the paths not only intersect, but do so along segments. Fortunately, the argument of *loc. cit.* used to circumvent this issue can be adapted to this setting. Namely, we perturb the vanishing paths $\gamma_{m,n}$ slightly to $\gamma'_{m,n}$ so that they no longer intersect along their radial segments. In addition, for those vanishing cycles whose corresponding vanishing path has radial segment greater than 2π we alter the vanishing paths to go *outside* of the critical points to form $\gamma''_{m,n}$, although it can be shown in the same way as [HS20, Lemma 3.3] that this alteration has no effect on the corresponding vanishing cycle. Finally, we perturb the fibration slightly to separate the vanishing paths going to the origin, as well as those whose critical points correspond to the same critical value. This is summarised in the following proposition, whose proof follows *mutatis mutandis* from that of the maximally graded case given in [HS20, Proposition 3.4].

⁶Note that we have reversed the orientation of the diagram in comparison to [Hab22, Figure 2] so that the orientation of the surface agrees with the orientation of the page.

Proposition 3.4. *There exists a perturbation of $\tilde{\mathbf{w}}_\varepsilon$ and a distinguished basis of vanishing paths such that the corresponding vanishing cycles are arbitrarily small perturbations of the ${}^{m,n}V_0^{\text{pr}}$, ${}^mV_{\mu_1\check{w}_1}$, ${}^nV_{\lambda_\ell\check{w}_\ell}$ and $V_{\lambda_i\mu_i}$ for $0 \leq m, M \leq \frac{p-1}{\ell} - 1$, $0 \leq n, N \leq q - 2$ as constructed above. The ${}^{m,n}V_0^{\text{pr}}$ are ordered by decreasing value of $\theta_{m,n}$, and by choosing the starting direction for our clockwise ordering to be $e^{i\theta}$, for θ a small positive angle, they occur before all of the other vanishing cycles. \square*

3.6. Isotoping the vanishing cycles and computing the morphisms. Now that we have constructed a distinguish basis of vanishing paths, we must compute the relevant Floer cohomology groups. In order to do this, we must Hamiltonian isotope the Lagrangians in the smooth fibre so that they intersect transversally. Fortunately, two Lagrangians only intersect non-transversally in the case of ${}^{m,n}V_0$ and ${}^{M,N}V_0$ where $m = M$ or $n \equiv N \pmod{\frac{q-1}{\ell}}$, where they intersect along segments. This is clear from the description of ${}^{m,n}V_0$ and ${}^{M,N}V_0$ in Σ' as $f_{m,n}(0,0)V_0$ and $f_{M,N}(0,0)V_0$, respectively. After describing the relevant perturbations, we will have constructed the final vanishing cycles which we will use to compute $\mathcal{A}_{\tilde{\Gamma}}^\vee$.

We begin by describing the isotopies of the Lagrangians on the λ_1 -axis. Namely, to achieve transversality, we isotope each ${}^{m,n}V_0$ anticlockwise in the λ_1 direction between the two necks by an amount proportional to n , correspondingly altering the curve at the boundaries of the neck region to keep the curve continuous. To make this isotopy Hamiltonian, we push the curve the corresponding amount in the clockwise direction around the $V_{\lambda_1\mu_1}$ neck region. The picture in this case is essentially [HS20, Figure 8].

To achieve transversality in the μ_ℓ plane, we perform essentially the same procedure as above, and of that in the maximally graded case; however, here we isotope the curves in the anticlockwise μ_ℓ direction by an amount proportional to $m + \frac{p-1}{\ell}\lfloor\frac{n\ell}{q-1}\rfloor$ in the region between the two necks, and then the curve is pushed clockwise in the $V_{\lambda_\ell\mu_\ell}$ neck region to compensate and make the isotopy Hamiltonian. See Figure 4 for an example⁷.

The resulting set of vanishing cycles, ${}^{m,n}V_0$, are then pairwise disjoint, except on the $V_{\lambda_i\mu_i}$ neck regions, where they are either disjoint or intersect transversally. Moreover, we will see momentarily that all of these intersection points are graded in degree 0, meaning that the differential on the Floer complex vanishes, and all intersection points survive to cohomology. Once this has been shown, it is then straightforward to see that, additively, the objects in $\mathcal{A}_{\tilde{\Gamma}}^\vee$ match that of \mathcal{B} via

$$\begin{aligned} {}^{m,n}V_0 &\leftrightarrow {}^{i,j}K_0 \\ {}^mV_{\mu_\ell\check{w}} &\leftrightarrow {}^iK_x[3] & \text{with } i+m = p-1 \\ {}^nV_{\lambda_1\check{w}} &\leftrightarrow {}^jK_y[3] & j+n = q-1. \\ V_{\lambda_r\mu_r} &\leftrightarrow K_{w_r}[3] \end{aligned} \tag{12}$$

All that is left to do to complete the theorem is show that the objects are graded and compose in the claimed way.

3.7. Composition. Suppose L_0 , L_1 and L_2 are three (final) vanishing cycles such that $L_0 < L_1 < L_2$ with respect to the ordering on the category $\mathcal{A}_{\tilde{\Gamma}}^\vee$ (we are calling them L rather than V to avoid conflict with our earlier notation for specific cycles). We need to compute the composition

$$HF^*(L_1, L_2) \otimes HF^*(L_0, L_1) \rightarrow HF^*(L_0, L_2), \tag{13}$$

which is defined by counting pseudo-holomorphic triangles, and Seidel [Sei08, Section (13b)] shows that, in the exact setting, this can be done combinatorially by counting triangular regions bounded by the L_i . In our non-exact setting, the assumptions of Section 3.1 ensure that the situation at

⁷The construction of this smooth fibre from gluing cylinders and strips is not the one given in [Hab21, Section 7.1.1], although is equivalent to this, since it results from a different choice representative of nodes in the construction of the quotient ribbon graph in *loc. cit.*

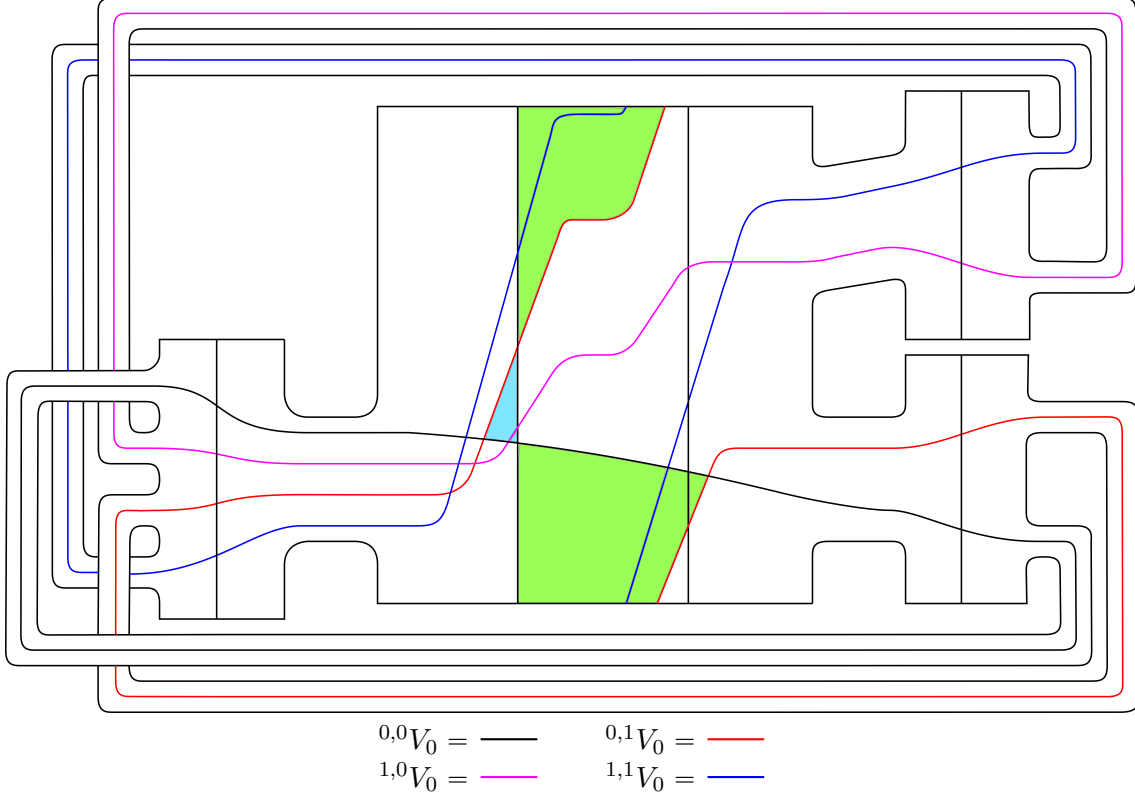


FIGURE 4. Smooth fibre with vanishing cycles for $\check{w} = x^5y + y^3x$. Top and bottom of each cylinder are identified. The light green and light blue triangles contribute to the relation corresponding to (iii) in Figure 1 since their areas are not equal.

hand is similarly combinatorial.

By the ordering on the vanishing cycles, the only possibility for (13) to be non zero is if $L_0 = {}^{m,n}V_0$ and $L_2 = {}^{M,N}V_0$ where either $m \geq M$ and $n \geq N$ or $M < m$ and $n \geq N + \frac{q-1}{\ell}$. There are then four possibilities for L_2 which would potentially give a non-zero composition:

- (i) $L_2 = V_{\lambda_i \mu_i}$ for some $i = 1, \dots, \ell$,
- (ii) $L_2 = {}^t V_{\lambda_1 \check{w}}$, for $t \equiv n \pmod{\frac{q-1}{\ell}}$
- (iii) $L_2 = {}^m V_{\mu_\ell \check{w}}$,
- (iv) $L_2 = {}^{r,s}V_0$ for some $(r, s) \neq (M, N)$ and either
 - (a) $M \geq r$ and $N \geq s$, or
 - (b) $M < r$ and $N \geq s + \frac{q-1}{\ell}$.

In the cases (ii) and (iii), there is a single obvious holomorphic disc contributing to the product, regardless of the ranks of the cohomology groups, and this is shown to be the only such disc by the same methods as in the maximally graded case; however, the case (i) and (iv) are more complicated. In case (i), there are $\text{rank}_{\mathbb{C}} HF^*({}^{m,n}V_0, {}^{M,N}V_0)$ holomorphic triangles contributing to (13), where the image of each is a scalar multiple of the intersection point ${}^{M,N}V_0 \pitchfork V_{\lambda_i \mu_i}$. The fact that this is all such maps follows from the same argument as in the maximally graded case, although where L_\cup is now three circles, one of which intersects the other two circles once, and two circles intersect each other $\text{rank}_{\mathbb{C}} HF^*({}^{m,n}V_0, {}^{M,N}V_0)$ times. Note that the vanishing cycles under consideration are all linearly independent in $H_1(\Sigma; \mathbb{Z})$ since the only vanishing cycles which are homologous are the $V_{\lambda_i \mu_i}$. This yields the analogue of the third relation in Figure 1, and is depicted in Figure 4. Composition in case (iv) is argued in the same way as case (i), yielding the analogue of the first relation in Figure 1. The last thing to check is that the signs of the morphisms can all be taken to be positive, which follows by the same argument as in Section 3.7 of the maximally graded case. (The spin structures

here are similarly the non-trivial ones.)

From this, we conclude:

Proposition 3.5. *There is a model for $\mathcal{A}_{\tilde{\Gamma}}$ which, under the identification (12), is described by the quiver in Figure 1 up to yet-to-be-determined gradings.* \square

3.8. Gradings and completion of proof. By construction, the morphisms in the B–model are graded, and the final piece of the puzzle is how to grade the Floer cohomology groups so that $\mathcal{A}_{\tilde{\Gamma}}$ matches \mathcal{B} as a graded algebra. Recall ([Sei00]) that a symplectic manifold (X, ω) is *gradable* if $K_X^{\otimes 2} \simeq \mathcal{O}_X$, and a grading is a choice of such trivialisation. This is possible if and only if $2c_1(X) = 0$, and so, in particular, all Calabi–Yau manifolds are gradable. Given a trivialising section $\Theta \in \Gamma(X, K_X^{\otimes 2})$, there is a map

$$\begin{aligned} \alpha_X : \mathrm{LGr}(TX) &\rightarrow S^1 \\ L_x &\mapsto \arg(\Theta|_{L_x}). \end{aligned}$$

For any Lagrangian $L \hookrightarrow X$, there is a natural map $L \rightarrow \mathrm{LGr}(TX)$ given by taking the class of the tangent space of L at each point, and we say that L is *gradable* with respect to the grading on X if the map $L \rightarrow \mathrm{LGr}(TX) \xrightarrow{\alpha_X} S^1$ lifts to a map $\alpha_L^\# : L \rightarrow \mathbb{R}$. This is possible if and only if the Maslov class of L vanishes, i.e. the map $L \rightarrow S^1$ is homotopic to the identity.

For Σ a real 2-dimensional manifold, i.e. a surface, gradings correspond naturally to line fields [Sei08, Section 13(c)], meaning a section of $\mathbb{P}_{\mathbb{R}}(T\Sigma) \simeq \mathrm{LGr}(T\Sigma)$. To see this, suppose that a grading on Σ has been chosen such that α_Σ is as above. Then, $\alpha_\Sigma^{-1}(1) = \eta$ is a line field. Conversely, given a line field η , one can construct α_Σ as above by measuring the anticlockwise angle between η_x and $L_x \in \mathrm{LGr}(T_x \Sigma)$. Given a line field grading Σ , a Lagrangian $\gamma : S^1 \rightarrow \Sigma$ is gradable with respect to this line field if and only if $\gamma^*\eta$ and γ^*TL are homotopic in $\gamma^*\mathbb{P}_{\mathbb{R}}(T\Sigma)$. Given a graded surface Σ with two graded Lagrangians $\alpha_{L_i}^\# : L_i \rightarrow \mathbb{R}$ for $i = 0, 1$, [Sei08, Example 11.20] shows that a transverse intersection point $x \in L_0 \pitchfork L_1$ has degree

$$|\alpha_{L_1}^\#(x) - \alpha_{L_0}^\#(x)| + 1$$

in $CF^*(L_0, L_1)$.

In our situation, the required choice of grading is the one which restricts to Σ from the grading of \tilde{X} . By the crepancy of the resolution π , this has vanishing first Chern class, and, since \tilde{X} is diffeomorphic to the Milnor fibre of $x^2 + y^2 + z^\ell$, its homotopy type is a bouquet of 2-spheres. This implies that \tilde{X} has vanishing first cohomology, and, in particular, there is a unique choice of trivialisation of $K_{\tilde{X}}^{\otimes 2}$ up to homotopy. We are therefore justified in the use of the definitive article when talking about gradings of \tilde{X} . Restricting the trivialisation of $K_{\tilde{X}}^{\otimes 2}$ to Σ uniquely determines the grading on Σ with respect to which our Lagrangians are graded. In particular, in the presentation of the smooth fibre as being glued from annuli given in [Hab21, Section 7.1.1], the line field is approximately horizontal on each annulus, and is approximately parallel to the boundary along each attaching strip.

As in the maximally graded case, we can grade the Lagrangians such that $\alpha_{L_i}^\#$ is valued between 0 and 1/2. Moreover, if $i > j$ in the ordering on the vanishing cycles given in Proposition 3.4, then $1/2 > \alpha_{L_i}^\# > \alpha_{L_j}^\# > 0$, and so all intersection points are graded in degree zero. Putting this all together, we arrive at the main theorem in the loop case, whose proof follows by the same argument as [HS20, Theorem 1], now that we have set it up.

Theorem 3.6 (Theorem 1, loop polynomial case). *Under (12), the \mathbb{Z} -graded A_∞ -category $\mathcal{A}_{\tilde{\Gamma}}$ is described by the quiver with relations in Figure 1 and is formal. In particular, by Theorem 2.7 it is quasi-equivalent to \mathcal{B} , and hence there is an induced quasi-equivalence*

$$\mathrm{mf}(\mathbb{C}^2, \Gamma, \mathbf{w}) \simeq \mathcal{FS}(\tilde{\mathbf{w}}).$$

4. CHAIN B-MODEL

In this section, we study the dg-category of L -graded matrix factorisations of $\mathbf{w} = x^p y + y^q$, where L this time is freely generated by \vec{x} and \vec{y} modulo the relation

$$\frac{p}{\ell} \vec{x} = \frac{q-1}{\ell} \vec{y},$$

where $\ell \leq d = \gcd(p, q-1)$ is again the index of Γ in $\Gamma_{\mathbf{w}}$. Analogously to the loop case, we consider $S = \mathbb{C}[x, y]$ as an L -graded ring with $|x| = \vec{x}$ and $|y| = \vec{y}$, so that \mathbf{w} is quasihomogeneous of degree \vec{c} , and write $R = S/(\mathbf{w})$. Similarly to the loop case, R is a graded Gorenstein ring of Krull dimension one and Gorenstein parameter $\alpha = \vec{x} + \vec{y} - \vec{c}$.

Analogously to the loop case, we write $\mathbf{w} = yw_1 \dots w_\ell$, where

$$w_r = x^{\frac{p}{\ell}} - e^{\frac{\pi\sqrt{-1}}{\ell}} \eta^r y^{\frac{q-1}{\ell}}$$

for η a primitive ℓ^{th} root of unity. With this, there are $\ell + 1$ matrix factorisations coming from (Γ -equivariantly) factoring \mathbf{w} . These correspond to

$$K_y^\bullet = (\dots \rightarrow S(-\vec{c}) \xrightarrow{w} S(-\vec{y}) \xrightarrow{y} S \rightarrow \dots),$$

as well as the matrix factorisations

$$K_{w_r}^\bullet = (\dots \rightarrow S(-\vec{c}) \xrightarrow{\mathbf{w}/w_r} S(-\frac{p}{\ell} \vec{x}) \xrightarrow{w_r} S \rightarrow \dots).$$

In addition, we also consider the objects

$${}^j K_y = K_y((j+1-q)\vec{y})$$

for $j = q - \frac{q-1}{\ell}, \dots, q-1$. Similarly to the loop case, for $1 \leq i \leq p-1$, $q - \frac{q-1}{\ell} \leq j \leq q-1$ and $k = \lfloor \frac{(i-1)\ell}{p} \rfloor$ we write

$$I_{i,j} = (x^i, x^{i-\frac{p}{\ell}} y^{j-(\ell-1)\frac{q-1}{\ell}}, \dots, x^{i-k\frac{p}{\ell}} y^{j-(\ell-k)\frac{q-1}{\ell}}, y^{j-(\ell-k-1)\frac{q-1}{\ell}})$$

and the L -graded R -modules

$$R(i\vec{x} + (j+1)\vec{y})/I_{i,j}.$$

The corresponding rank $(k+2)$ matrix factorisation, which we denote by ${}^{i,j} K_0$, is given by stabilising this module beginning with

$$R((j+1)\vec{y}) \oplus \bigoplus_{t=0}^{k-1} R(\vec{c}) \oplus R(\vec{c} + i\vec{x} - (k+1)\frac{q-1}{\ell}\vec{y}) \xrightarrow{(x^i \quad \dots \quad y^{j-(\ell-k-1)\frac{q-1}{\ell}})} R(i\vec{x} + (j+1)\vec{y}).$$

From this, it is straightforward to check that maps defining the matrix factorisation are given in even degree by

$$d_0 = \begin{pmatrix} y^{j-(\ell-1)\frac{q-1}{\ell}} & 0 & \dots & 0 & x^{p-i}y \\ -x^{\frac{p}{\ell}} & y^{\frac{q-1}{\ell}} & \dots & 0 & 0 \\ 0 & -x^{\frac{p}{\ell}} & \dots & 0 & 0 \\ 0 & 0 & \dots & 0 & 0 \\ \vdots & \vdots & \ddots & \vdots & \vdots \\ 0 & 0 & \dots & y^{\frac{q-1}{\ell}} & 0 \\ 0 & 0 & \dots & -x^{i-k\frac{p}{\ell}} & y^{q-j+(\ell-k-1)\frac{q-1}{\ell}} \end{pmatrix}, \quad (14)$$

and in odd degree by $d_1 = \text{Adj}(d_0)$. Explicitly, we have that ${}^{i,j} K_0$ corresponds to the matrix factorisation

$$\begin{array}{ccccccc}
S(\vec{c} - \frac{q-1}{\ell} \vec{y}) & & S((j+1)\vec{y}) & & S(2\vec{c} - \frac{q-1}{\ell} \vec{y}) & & \\
\oplus & & \oplus & & \oplus & & \\
\cdots & \oplus_{t=0}^{k-1} S(\vec{c} - \frac{q-1}{\ell} \vec{y}) & \xrightarrow{d_0} & \oplus_{t=0}^{k-1} S(\vec{c}) & \xrightarrow{d_1} & \oplus_{t=0}^{k-1} S(2\vec{c} - \frac{q-1}{\ell} \vec{y}) & \cdots \\
& \oplus & & \oplus & & & \\
& S((j+1)\vec{y} + i\vec{x} - \vec{c}) & & S(\vec{c} + i\vec{x} - (k+1)\frac{q-1}{\ell} \vec{y}) & & S((j+1)\vec{y} + i\vec{x}) &
\end{array}$$

where, as before, the rightmost term is in cohomological degree 0.

As in the maximally graded and loop cases case, we are interested in a full subcategory \mathcal{B} of $\text{mf}(\mathbb{C}^2, \Gamma, \mathbf{w})$ consisting of the objects described above. Namely, let \mathcal{B} be the category consisting of the $\frac{p(q-1)}{\ell} + \ell$ objects

$$V = \{{}^{i,j}K_0, {}^jK_y, K_{w_1}[3], \dots, K_{w_\ell}[3]\}_{i=1, \dots, p-1; j=q-\frac{q-1}{\ell}, \dots, q-1}.$$

In the following sections we compute the morphisms between the objects in this category, culminating in the description of \mathcal{B} as a quiver algebra in Theorem 4.4.

4.1. Morphisms between the K_x 's, K_y 's and K_{w_r} 's. For calculations regarding the modules K_y and K_{w_r} , the arguments carry over from the maximally graded and loop cases with minimal alteration.

Lemma 4.1. *In $\text{HMF}(\mathbb{C}^2, \Gamma, \mathbf{w})$, we have the following:*

- (i) *For any $j \in \mathbb{Z}$, the objects ${}^jK_y, \dots, {}^{j+\frac{q-1}{\ell}-1}K_y$ are exceptional and pairwise orthogonal.*
- (ii) *The objects $K_{w_1}, \dots, K_{w_\ell}$ are exceptional pairwise orthogonal*
- (iii) *For each $j = q - \frac{q-1}{\ell}, \dots, q-1$ and $r = 1, \dots, \ell$, the objects jK_y and K_{w_r} are mutually orthogonal.* \square

4.2. Morphisms between the K_w 's and K_0 's. The fact that $\text{Hom}^\bullet(K_{w_r}, {}^{i,j}K_0) = 0$ is routine. In the other direction, we argue as in the loop case. Namely, we observe that

$$\dim_{\mathbb{C}} \text{Hom}^\bullet(K_{w_r}, {}^{i,j}K_0(\vec{c} - \vec{x} - \vec{y})) = \begin{cases} 1 & \text{if } \bullet = -3 \\ 0 & \text{otherwise,} \end{cases} \quad (15)$$

and then find a non-trivial element of $\text{Hom}^3({}^{i,j}K_0, K_{w_r})$. This results in the following lemma, whose proof is easily adapted from that of Lemma 2.4.

Lemma 4.2. *For each $r = 1, \dots, \ell$, there is a single morphism between ${}^{i,j}K_0$ and K_{w_r} given by*

$$\text{Hom}^3({}^{i,j}K_0, K_{w_r}) = \mathbb{C} \cdot \begin{pmatrix} y^{q-1-j} \\ e^{-\frac{\pi i}{\ell}} \eta^{-r} \\ (e^{-\frac{\pi i}{\ell}} \eta^{-r})^2 \\ \vdots \\ (e^{-\frac{\pi i}{\ell}} \eta^{-r})^k \\ (e^{-\frac{\pi i}{\ell}} \eta^{-r})^{k+1} x^{(k+1)\frac{p}{\ell} - i} \end{pmatrix}.$$

\square

Computing morphisms ${}^{i,j}K_0 \rightarrow {}^{I,J}K_0$ is analogous to the maximally graded case, and follows the argument of Section 2.3. Namely, morphisms ${}^{i,j}K_0 \rightarrow {}^{I,J}K_0$ are spanned by the module

$$(R/I_{I,J})_{(I-i)\vec{x} + (J-j)\vec{y}}$$

in degree zero. From this, it is immediate that there are no morphisms unless $I \geq i$. Analogously to the loop case, it is now possible to have $j > J$ since $\frac{p}{\ell}\vec{x} = \frac{q-1}{\ell}\vec{y}$. Putting this together, we conclude:

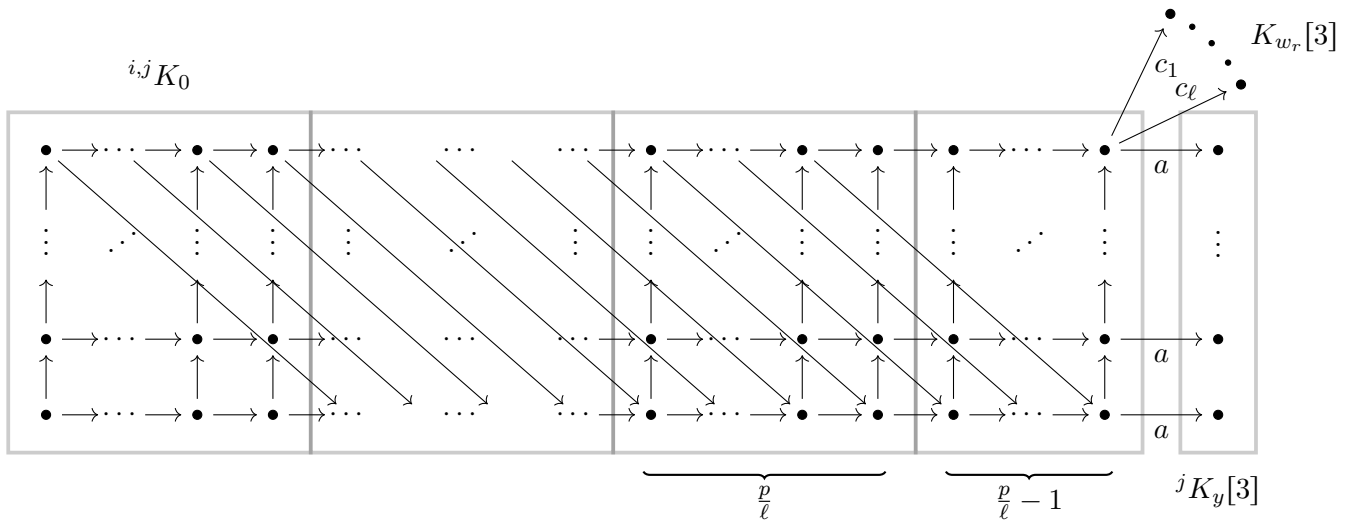
Lemma 4.3. *For all $i \in \{1, \dots, p-1\}$ and $j \in \{q - \frac{q-1}{\ell}, \dots, q-1\}$, we have*

$$\text{Hom}^\bullet({}^{i,j}K_0, {}^{I,J}K_0) \simeq \begin{cases} \text{span}\{x^{I-i}y^{J-j}, \dots, x^{(I-i) \bmod \frac{p}{\ell}}y^{J-j+k\frac{q-1}{\ell}}\} & \text{if } I \geq i, J \geq j \\ \text{span}\{x^{I-i-\frac{p}{\ell}}y^{J-j+\frac{q-1}{\ell}}, \dots, x^{(I-i) \bmod \frac{p}{\ell}}y^{J-j+k\frac{q-1}{\ell}}\} & \text{if } J < j, I \geq i + \frac{p}{\ell} \\ 0 & \text{otherwise.} \end{cases}$$

\square

4.3. The total endomorphism algebra of the basic objects. As in the loop case, we are able to describe the endomorphism algebra of the category \mathcal{B} explicitly as a quiver-with-relations. The proof follows from that of the maximally graded case with the analogous alterations required in Theorem 2.7.

Theorem 4.4. *The cohomology-level total endomorphism algebra of the objects of \mathcal{B} is the algebra of the quiver-with-relations described in Figure 5, with all arrows living in degree zero. In particular, \mathcal{B} is a \mathbb{Z} -graded A_∞ -category concentrated in degree 0, so is intrinsically formal.*



Morphisms:

- (i) Horizontal arrows are labelled by x ,
- (ii) Vertical and diagonal arrows are labelled by y .

Relations:

- (i) $xy = yx$,
- (ii) $ay = 0$,
- (iii) $c_r(x^{\frac{p}{\ell}} - e^{\frac{\pi i}{\ell}} \eta^r y^{\frac{q-1}{\ell}}) = 0$.

FIGURE 5. The quiver describing the category \mathcal{B} for chain polynomials.

4.4. Generation. The last step in showing that the collection of objects in \mathcal{B} generates $\text{mf}(\mathbb{C}^2, \Gamma, \mathbf{w})$.

Proposition 4.5. *The functor*

$$\text{Tw } \mathcal{B} \rightarrow \text{mf}(\mathbb{C}^2, \Gamma, \mathbf{w})$$

is a quasi-equivalence.

Proof. The strategy is the same as Proposition 2.11, so we will be brief, only explaining the points which differ from the loop and maximally graded chain cases. As before, we must prove that $R(l)/(x, y) \in \langle V \rangle$ for each $l \in L/\bar{c}\mathbb{Z} \simeq \mathbb{Z}/(\frac{pq}{\ell})$, and we begin by observing that $R(a\vec{x}+b\vec{y})/(x, y) \in \langle V \rangle$ for $a = 1, \dots, p-1$, $b = q+1 - \frac{q-1}{\ell}$ by the same argument as in the loop and maximally graded cases. Furthermore, we see that, up to grading shifts by $[-2]$, this includes $R(l\vec{y})/(x, y)$ for $l = 1, \dots, (\ell-1)\frac{q-1}{\ell}$, as well as $R((a-\frac{p}{\ell})\vec{x}+\vec{y})/(x, y)$ for $a = 1, \dots, p-1$. From the $R(l\vec{y})/(x, y)$, we build $R(l\vec{y})/(y)$

for $l = 1, \dots, (\ell-1)\frac{q-1}{\ell}$, which, together with the grading shifts of ${}^j K_y$, show that $R(l\vec{y})/(y) \in \langle V \rangle$ for all $l \in \mathbb{Z}$ except for $l \equiv -\frac{q-1}{\ell} \pmod{\vec{c}}$. We build this module analogously to $R((p - \frac{p-1}{\ell})\vec{x} + \vec{y})/(xy)$ in the loop case. Namely, we observe that $K_{w_1}[1] = R((q - \frac{q-1}{\ell})\vec{y})/(yw_2 \dots w_\ell)$, and construct $R((q - \frac{q-1}{\ell})\vec{y})/(y)$ by iteratively taking cones

$$R((r-1)\frac{q-1}{\ell}\vec{y})/(w_r) \xrightarrow{yw_{r+1} \dots w_\ell} R((q - \frac{q-1}{\ell})\vec{y})/(yw_r \dots w_\ell)$$

for $r = 2, \dots, \ell$. The modules $R(l\vec{y})/(w_r)$ for any $l = 1, \dots, (\ell-1)\frac{q-1}{\ell}$ and $r = 1, \dots, \ell$ are constructed as the cone of

$$R((l - \frac{q-1}{\ell})\vec{y})/(y) \xrightarrow{w_r} R(l\vec{y})/(yw_r),$$

where the module in the codomain is given by the cone of $R((l-1)\vec{y})/(y) \xrightarrow{y} R(l\vec{y})/(yw_1)$. Now that we have constructed modules $R(l\vec{y})/(y)$ for all $l \in \mathbb{Z}$, we can produce $R(l\vec{y})/(x, y)$ for any $l = 1, \dots, q-1$ as in the maximally graded case. Then, all that is left to do is construct $R/(x, y)$ and $R(ax + y)$ for $a = p - \frac{p}{\ell} + 1, \dots, p-1$. The latter modules are constructed similarly to the maximally graded by observing that the cone of the morphism

$$\bigoplus_{t=0}^{\ell-1} R/(w) \xrightarrow{(x^i \dots x^{i-(\ell-1)\frac{p}{\ell}} y^{(\ell-1)\frac{q-1}{\ell}})} R(i\vec{x})/(w)$$

is ${}^{i,q-1}K_0$, and so $R(i\vec{x})/(w)[1] = R(i\vec{x} + \vec{y})/(y) \in \langle V \rangle$. From here, the proof proceeds as in the maximally graded case. \square

We deduce the following corollary, whose proof follows from Proposition 4.5 and Theorem 4.4 in the same way as in the proof of [HS20, Theorem 4.9]:

Corollary 4.6 (Corollary 1, chain polynomial case). *The object*

$$\mathcal{E} := \left(\bigoplus_{\substack{i=1, \dots, p-1 \\ j=q-\frac{q-1}{\ell}, \dots, q-1}} {}^{i,j}K_0 \right) \oplus \left(\bigoplus_{j=q-\frac{q-1}{\ell}, \dots, q-1} {}^jK_y[3] \right) \oplus \left(\bigoplus_{r=1, \dots, \ell} K_{w_r}[3] \right)$$

is a tilting object for $\text{mf}(\mathbb{C}^2, \Gamma, \mathbf{w})$.

5. CHAIN A-MODEL

In this section, we characterise the Fukaya–Seidel category of $\check{\mathbf{w}} = \check{x}^p + \check{x}\check{y}^q$ with symmetry group $\check{\Gamma}$ not necessarily trivial. The content of Section 3.1 applies to this section unaltered, and the subsequent subsections essentially follow from applying the same alterations of the maximally graded case as was needed to study the loop A-model.

5.1. A resonant Morsification. As in the maximally graded and loop cases, we introduce the Morsification $\check{\mathbf{w}}_\varepsilon = \check{x}^p + \check{x}\check{y}^q - \varepsilon\check{x}\check{y}$, and observe that it descends to $\check{\mathbf{w}}_\varepsilon : X \rightarrow \mathbb{C}$ as

$$\check{\mathbf{w}}_\varepsilon(u, v, w) = u^{\frac{p}{\ell}} + wv^{\frac{q-1}{\ell}} - \varepsilon w.$$

Pulling this back to the chart \tilde{X}_i , we get

$$\check{\mathbf{w}}_i(\lambda_i, \mu_i) = \lambda_i^{\frac{pi}{\ell}} \mu_i^{\frac{(i-1)p}{\ell}} + \lambda_i^{\frac{(\ell-i)(q-1)}{\ell}+1} \mu_i^{\frac{(\ell+1-i)(q-1)}{\ell}+1} - \varepsilon \lambda_i \mu_i,$$

where we continue to suppress the ε from the notation when considering $\check{\mathbf{w}}_\varepsilon : \tilde{X} \rightarrow \mathbb{C}$ on charts. Each $\check{\mathbf{w}}_i$ is similarly tame in the sense of [Bro88].

The first thing to notice is that, when $p = \ell = 2$ and $q = 2n + 1$, $\check{\mathbf{w}}_\varepsilon$ is only singular on one of the charts, where it is given by the loop polynomial with $p = 2$ and $q = n + 1$, and we can compute the Fukaya–Seidel categories using previous results. This observation actually constitutes part of

the initial evidence of the conjecture of Futaki and Ueda, where they observed that, when $n = 1$, the corresponding category is the derived category of modules on the D_4 quiver. Since the A-model reduces to the maximally graded loop case when $p = \ell = 2$, we will restrict ourselves to the case $p > 2$ in what follows.

Remark 5.1. Unlike in the loop case, the smooth fibre of $\tilde{\mathbf{w}}$ is no longer described by any $\tilde{\mathbf{w}}_i^{-1}(-\delta)$. Namely, the line $\{\mu_1 = 0\} \subseteq \tilde{\mathbf{w}}_1^{-1}(-\delta)$ in the first chart is only described in this chart. In particular, whilst the Fukaya–Seidel category for the case $p = 2, q = 3$ described above matches that of $\check{x}^2\check{y} + \check{x}\check{y}^2$, the smooth fibre is the *twice* punctured torus, not the thrice punctured torus given by the Milnor fibre in the loop case. Nevertheless, the critical points of type (iii) below are equivalently described in any of the charts.

Remark 5.2. Continuing on from the above, it should be pointed out that the holomorphic curves contributing to the computation of the Fukaya–Seidel category of $\tilde{\mathbf{w}}$ when $p = 2$ do not pass through the line $\{\mu_1 = 0\}$ in \tilde{X}_1 , and so the category genuinely matches that of the maximally graded loop polynomial.

As before, the critical points are grouped into the following three types:

- (i) $\mu_\ell^{\frac{q-1}{\ell}} = \varepsilon, \lambda_\ell = 0$
- (ii) $\mu_i = \lambda_i = 0$ for $i = 1, \dots, \ell$
- (iii) $\mu_\ell^{\frac{q-1}{\ell}} = \frac{\varepsilon}{q}, \lambda_\ell^{p-1} = \frac{\varepsilon(q-1)}{pq} \mu_\ell^{1-\frac{(\ell-1)p}{\ell}}$.

the critical values of type (i) and (ii) are both 0, and the critical value corresponding to a critical point of type (iii) is

$$\frac{-\varepsilon\mu_\ell\lambda_\ell(p-1)(q-1)}{pq}.$$

Similarly to the loop case, there is a clear symmetry of these critical points. Namely, let $(\lambda_{\ell,\text{crit}}^+, \mu_{\ell,\text{crit}}^+)$ be the unique positive real critical point of type (iii) in the chart \tilde{X}_ℓ , with corresponding critical value c_{crit} . Letting ζ and η denote the roots of unity

$$\zeta = e^{2\pi i/(p-1)} \quad \text{and} \quad \eta = e^{2\pi i/(q-1)}, \tag{16}$$

as well as $\alpha = e^{2\pi i/(p-1)(q-1)}$, we see that there is a $\mu_{p-1} \times \mu_{q-1}$ action on the critical points of type (iii) given by

$$\{(\zeta^m \eta^{n(1-\ell)} \alpha^n \lambda_{\ell,\text{crit}}^+, \eta^{n\ell} \mu_{\ell,\text{crit}}^+) : 0 \leq m \leq p-2, 0 \leq n \leq q-2\}.$$

The critical value corresponding to $(\zeta^m \eta^{n(1-\ell)} \alpha^n \lambda_{\ell,\text{crit}}^+, \eta^{n\ell} \mu_{\ell,\text{crit}}^+)$ is $\alpha^{m(q-1)+np} c_{\text{crit}}$, so there are $\frac{\gcd(p,q-1)}{\ell}$ critical points in each of these critical fibres. We therefore restrict to the subset

$$\{(\zeta^m \eta^{n(1-\ell)} \alpha^n \lambda_{\ell,\text{crit}}^+, \eta^{n\ell} \mu_{\ell,\text{crit}}^+) : 0 \leq m \leq p-2, 0 \leq n \leq \frac{q-1}{\ell} - 1\}$$

in order to describe all of the critical points of type (iii) via symmetry.

The technical input and strategy for the chain case is identical to that of the loop case, with the only differences being superficial. We therefore keep this section brief, and only describe the alterations necessary in the chain case as they differ from the loop and maximally graded chain cases.

The vanishing paths corresponding to critical points (i) and (ii) are still straight lines from $-\delta$ to the origin, and we denote the corresponding vanishing cycles by ${}^n V_{\lambda_1 \tilde{w}_1}$ and $V_{\lambda_i \mu_i}$. The preliminary vanishing paths $\gamma_{m,n}$ are given by the circular arc from $-\delta e^{-\theta}$ as θ increases from 0 to

$$\theta_{m,n} = 2\pi \left(\frac{m}{p-1} + \frac{pn}{(p-1)(q-1)} \right),$$

and then the straight line path from $-\alpha^{m(q-1)+np}\delta$ to $\alpha^{m(q-1)+np}c_{\text{crit}}$. Again, we write ${}^{m,n}V_0^{\text{pr}}$ for the corresponding vanishing cycles.

5.2. The zero fibre and its smoothing. The fibre of $\check{\mathbf{w}}_\varepsilon$ above the origin has $\ell+1$ components. Namely, it comprises: the line $\{\lambda_\ell = 0\}$ in the chart \tilde{X}_ℓ , the planes $(0, \mu_i)$ and $(\lambda_{i+1}, 0)$ in the charts \tilde{X}_i and \tilde{X}_{i+1} , respectively, which patch together to give $\ell-1$ projective lines in an $A_{\ell-1}$ configuration, and the curve given by $\check{w}_i = \check{\mathbf{w}}_i \lambda_i^{-1} \mu_i^{-1}$ in the charts \tilde{X}_i for $i = 2, \dots, \ell$, and by $\check{w}_1 = \check{\mathbf{w}}_1 \lambda_1^{-1}$ in \tilde{X}_1 .

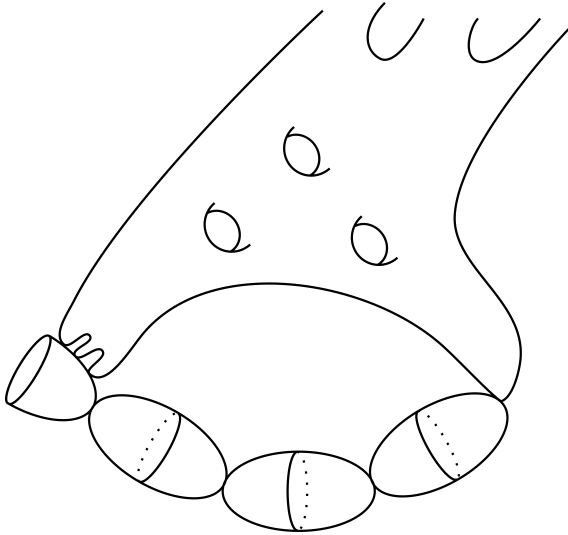


FIGURE 6. A sketch of the fibre of $\check{\mathbf{w}}_\varepsilon$ above the origin.

Remark 5.3. The topology of the smooth fibre was computed in [Hab21, Section 7.1.2]. Namely, it is a curve of genus

$$g(\Sigma) = \frac{1}{2\ell}(pq - p + \ell - \gcd(\ell q, p + q - 1))$$

with $1 + \gcd(q, \frac{p+q-1}{\ell})$ boundary punctures.

5.3. The vanishing cycles. Just as in the loop case, we first construct the real vanishing cycle ${}^{0,0}V_0^{\text{pr}}$ and then construct the rest by a combination of symmetry considerations and parallel transport. In this case, the symplectomorphism $f_{m,n}^{(i)}$ is given by

$$\begin{aligned} f_{m,n}^{(i)} : \tilde{X}_i &\rightarrow \tilde{X}_i \\ (\lambda_i, \mu_i) &\mapsto (\xi^{m(\ell+1-i)} \eta^{n(1-i)} \alpha^{n(\ell+1-i)} \lambda_i, \xi^{n(i-\ell)} \eta^{ni} \alpha^{n(i-\ell)} \mu_i). \end{aligned}$$

Applying the parallel transport arguments of the loop case, we see that the μ_i coordinate of the Lagrangian ${}^{m,n}V_0^{\text{pr}}$ interpolates between

$$-2\pi \left(\frac{m(q-1)(\ell+1-i) + np(1-i) + n\ell}{(p-1)(q-1)} \right) \quad \text{and} \quad 2\pi \left(\frac{m(i-\ell)(q-1) + nip - n\ell}{(p-1)(q-1)} \right)$$

in the neck region containing $V_{\lambda_i \mu_i}$ as $|\mu_\ell|$ increases, whilst the argument $\mu_\ell - \eta^{n\ell} \mu_{(\ell, \text{crit}^+)}$ interpolates the other way in its argument about the neck region containing ${}^n V_{\lambda_1 \check{w}_1}$.

As in the loop case, we modify the vanishing paths so that they are disjoint away from the distinguished point when the difference in the argument of the straight-line segments is less than 2π . We then push the remaining cycles to go outside outside of the critical points, and see that this does not affect the vanishing cycles. Correspondingly, we deduce the analogue of Proposition 3.4 in the chain case. We then Hamiltonian isotope the vanishing cycles in the distinguished fibre in

the same way as in the loop case (although we only need to do this on the neck regions in \tilde{X}_ℓ now), producing a collection of ordered and transversely intersecting Lagrangians with which we can compute $\mathcal{A}_{\tilde{\Gamma}}$.

5.4. Composition and gradings. We continue to present the smooth fibre as being glued from cylinders, and the line field used to grade this surface was given in [Hab21, Section 7.1.2]; namely, it is the line field which is approximately horizontal on each cylinder, and parallel to the attaching strips. With this grading, we have the proof of the main theorem in the chain case.

Theorem 5.4 (Theorem 1, chain polynomial case). *Under the correspondence*

$$\begin{aligned} {}^{m,n}V_0 &\leftrightarrow {}^{i,j}K_0 \\ {}^nV_{\lambda_1 \check{w}} &\leftrightarrow {}^jK_y[3] \quad \text{with} \quad \begin{cases} i+m = p-1 \\ j+n = q-1 \end{cases} \\ V_{\lambda_r \mu_r} &\leftrightarrow K_{w_r}[3] \end{aligned} \tag{17}$$

the \mathbb{Z} -graded A_∞ category $\mathcal{A}_{\tilde{\Gamma}}$ is identified with the quiver algebra of Theorem 4.4 and is formal, so there is a quasi-equivalence

$$\mathrm{mf}(\mathbb{C}^2, \Gamma, \mathbf{w}) \simeq \mathcal{FS}(\check{\mathbf{w}})$$

Proof. The only thing to check is that the morphisms in $\mathcal{A}_{\tilde{\Gamma}}$ compose in the claimed way, but this follows by the same reasoning in the loop case. \square

6. BRIESKORN–PHAM POLYNOMIALS

6.1. The B-model. We now deal with the last, and most simple, of invertible polynomials in two variables. Namely, we let $\mathbf{w} = x^p + y^q$, and consider the L -graded rings $S = \mathbb{C}[x, y]$ and $R = S/(\mathbf{w})$, where L is generated by $|x| = \vec{x}$ and $|y| = \vec{y}$ modulo the relations

$$\frac{p}{\ell} \vec{x} = \frac{q}{\ell} \vec{y},$$

where $\ell \leq d = \gcd(p, q)$ is the index of Γ in $\Gamma_{\mathbf{w}}$ so that $L \simeq \mathbb{Z} \oplus \mathbb{Z}/(\frac{d}{\ell})$ and \mathbf{w} is homogeneous of degree $\vec{c} = p\vec{x} = q\vec{y}$. Moreover, we have $L/\vec{c}\mathbb{Z} \simeq \mathbb{Z}/(\frac{pq}{d}) \times \mathbb{Z}/(\frac{d}{\ell})$. Similarly to the previous cases, we write $\mathbf{w} = w_1 \dots w_\ell$, where

$$w_r = x^{\frac{p}{\ell}} - e^{\frac{\pi\sqrt{-1}}{\ell}} \eta^r y^{\frac{q}{\ell}}$$

for η a primitive ℓ^{th} root of unity. With this, there are ℓ matrix factorisations coming from equivariantly factoring \mathbf{w}

$$K_{w_r}^\bullet = (\dots \rightarrow S(-\vec{c}) \xrightarrow{\mathbf{w}/w_r} S(-\frac{p}{\ell} \vec{x}) \xrightarrow{w_r} S \rightarrow \dots)$$

In the maximally graded case, this is the zero object in the category of matrix factorisations, but in the non-maximally graded case these give non-trivial objects. We will therefore assume from now on that $\ell > 1$, since the two cases are treated differently and the maximally graded case is already established as a special case of [FU11]. We assume without loss of generality that $p \geq q$.

The modules supported at the origin are the analogues of those in the loop and chain cases. Namely, we write $k = \lfloor \frac{(j-1)\ell}{q} \rfloor$, and consider the L -graded modules

$$R(i\vec{x} + j\vec{y})/(x^{i-(\ell-k-1)\frac{p}{\ell}}, x^{i-(\ell-k)\frac{p}{\ell}} y^{j-k\frac{q}{\ell}}, \dots, x^{i-(\ell-1)\frac{p}{\ell}} y^{j-\frac{q}{\ell}}, y^j)$$

for $i = (\ell-1)\frac{p}{\ell} + 1, \dots, p-1$ and $j = 1, \dots, q-1$, together with

$$R((\ell-1)\frac{p}{\ell} \vec{x} + j\vec{y})/(x^{k\frac{p}{\ell}}, x^{(k-1)\frac{p}{\ell}} y^{j-k\frac{q}{\ell}}, \dots, x^{\frac{p}{\ell}} y^{j-2\frac{q}{\ell}}, y^{j-\frac{q}{\ell}})$$

for $j = \frac{q}{\ell} + 1, \dots, q-1$. We let ${}^{i,j}K_0$ be the corresponding matrix factorisation, which, for the modules with $i > (\ell-1)\frac{p}{\ell}$ is given by

$$\begin{array}{ccc}
S(\vec{c} - \frac{p}{\ell} \vec{x}) & S(\vec{c} - (k+1) \frac{p}{\ell} \vec{x} + j \vec{y}) & S(2\vec{c} - \frac{p}{\ell} \vec{x}) \\
\oplus & \oplus & \oplus \\
\cdots & \xrightarrow{d_0} & \oplus_{t=0}^{k-1} S(\vec{c}) & \xrightarrow{d_1} & \oplus_{t=0}^{k-1} S(2\vec{c} - \frac{p}{\ell} \vec{x}) & \cdots \\
& \oplus & \oplus & & & \\
& S(i\vec{x} + j\vec{y} - \vec{c}) & S(i\vec{x}) & & S(i\vec{x} + j\vec{y}) &
\end{array}$$

where

$$d_0 = \begin{pmatrix} y^{j-k} \frac{q}{\ell} & 0 & 0 & \dots & 0 & x^{p-i+\frac{p}{\ell}(\ell-1-k)} \\ -x^{\frac{p}{\ell}} & y^{\frac{q}{\ell}} & 0 & \dots & 0 & 0 \\ 0 & -x^{\frac{p}{\ell}} & y^{\frac{q}{\ell}} & \dots & 0 & 0 \\ 0 & 0 & -x^{\frac{p}{\ell}} & \dots & 0 & 0 \\ \vdots & \vdots & \vdots & \ddots & \vdots & \vdots \\ 0 & 0 & 0 & \dots & y^{\frac{q}{\ell}} & 0 \\ 0 & 0 & 0 & \dots & -x^{i-(\ell-1)\frac{p}{\ell}} & y^{q-j} \end{pmatrix}, \quad (18)$$

and $d_1 = \text{Adj}(d_0)$. The matrix factorisations for $(\ell-1)\frac{p}{\ell}, j K_0$ are similar, although are of rank $k+1$. Analogously to the loop and chain cases, we consider the category \mathcal{B} whose objects are $R/(w_r)[3]$ for $r = 1, \dots, \ell$ and $i, j K_0$ above. Arguing as before, we arrive at:

Theorem 6.1. *The cohomology-level total endomorphism algebra of the objects of \mathcal{B} is the algebra of the quiver-with-relations described in Figure 7, with all arrows living in degree zero. In particular, \mathcal{B} is a \mathbb{Z} -graded A_∞ -category concentrated in degree 0, so is intrinsically formal.*

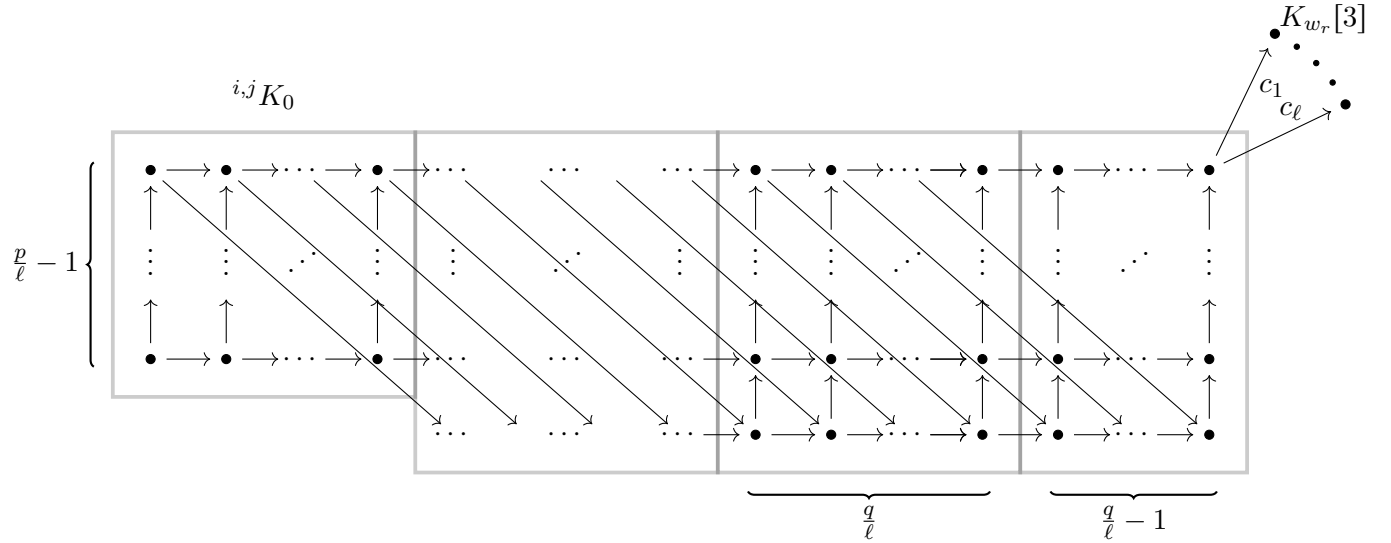


FIGURE 7. The quiver describing the category \mathcal{B} for Brieskorn–Pham polynomials.

As before, we claim that the collection of objects in \mathcal{B} generates $\text{mf}(\mathbb{C}^2, \Gamma, \mathbf{w})$; the proof follows the same strategy of Propositions 2.11 and 4.5.

Proposition 6.2. *The functor*

$$\mathrm{Tw} \mathcal{B} \rightarrow \mathrm{mf}(\mathbb{C}^2, \Gamma, \mathbf{w})$$

is a quasi-equivalence. \square

From this, we deduce the Corollary 1 in the Brieskorn–Pham case in the same way as in the loop and chain cases.

Corollary 6.3 (Corollary 1, Brieskorn–Pham polynomial case). *The object*

$$\mathcal{E} := \left(\bigoplus_{\substack{i=(\ell-1)\frac{p}{\ell}, \dots, p-1 \\ j=2, \dots, q-1}} {}^{i,j} K_0 \right) \oplus \left(\bigoplus_{i=(\ell-1)\frac{p}{\ell}+\frac{q}{\ell}, \dots, p-1} {}^{i,j} K_0 \right) \oplus \left(\bigoplus_{r=1, \dots, \ell} K_{w_r}[3] \right)$$

is a tilting object for $\mathrm{mf}(\mathbb{C}^2, \Gamma, \mathbf{w})$.

6.2. The A-model. The computation of the A-model for Brieskorn–Pham polynomials is, by this point, routine. The argument follows the previous two cases, and so we only summarise the results here. For a Brieskorn–Pham polynomial $\tilde{\mathbf{w}} = \check{x}^p + \check{y}^q$, we have $d = \gcd(p, q)$, and we again Morsify as $\tilde{\mathbf{w}}_\varepsilon = \check{x}^p + \check{y}^q - \varepsilon \check{x} \check{y}$. This descends to \mathbb{C}^2/μ_ℓ as $\tilde{\mathbf{w}} = u^{\frac{p}{\ell}} + v^{\frac{q}{\ell}} - \varepsilon w$, and pulls back to the chart \tilde{X}_i as

$$\tilde{\mathbf{w}}_i(\lambda_i, \mu_i) = \lambda_i^{\frac{p}{\ell}} \mu_i^{\frac{(i-1)p}{\ell}} + \lambda_i^{\frac{(\ell-i)q}{\ell}} \mu_i^{\frac{(\ell+1-i)q}{\ell}} - \varepsilon \lambda_i \mu_i.$$

The critical values fall into the groups

- (i) $\mu_i = \lambda_i = 0$ for $\begin{cases} i = 1, \dots, \ell & \text{if } q > \ell, \\ i = 1, \dots, \ell-1 & \text{if } p > q = \ell, \\ i = 2, \dots, \ell-1 & \text{if } p = q = \ell, \end{cases}$
- (ii) $\mu_\ell = 0, \lambda_\ell = \frac{1}{\varepsilon}$ if $p > q = \ell$
- (iii) $\mu_\ell = 0, \lambda_\ell = \frac{1}{\varepsilon}$ and $\lambda_1 = 0, \mu_1 = \frac{1}{\varepsilon}$ if $p = q = \ell$
- (iv) $\mu_1^{q-1} = \frac{\varepsilon}{q} \lambda_1^{1-\frac{(\ell-1)q}{\ell}}, \lambda_1^{\frac{p}{\ell}-1} = \frac{\varepsilon \mu_1}{p}$.

The critical value corresponding to critical points in the first three groups is zero, whilst the $\frac{(p-1)(q-1)-1}{\ell}$ critical points in the second group have critical value

$$\frac{-\varepsilon \mu_1 \lambda_1 ((p-1)(q-1)-1)}{pq}.$$

The situation where $p > q = \ell$ or $p = q = \ell$ is essentially the same as the cases where $q > \ell$, and we will denote the vanishing cycles corresponding to the critical points of type (ii) and (iii), when they are relevant, as $V_{\lambda_\ell \mu_\ell}$ and $V_{\lambda_1 \mu_1}$. The difference is seen in Figure 8, where the component of the fibre above zero corresponding to $\tilde{\mathbf{w}}_i \lambda_i^{-1} \mu_i^{-1}$ for $i \neq 1, \ell$ doesn't intersect the exceptional locus at the origin of \tilde{X}_j for $j = 1, \ell$. This is a topologically irrelevant difference, and we treat the critical points of type (ii) and (iii) in the same way as those of type (i).

As before, we denote $(\lambda_{1,\mathrm{crit}}^+, \mu_{1,\mathrm{crit}}^+)$ the unique positive real critical point whose critical value is c_{crit} . The other critical points are then attained by symmetry considerations. Namely, for

$$(m, n) \in (\{0, \dots, p-2\} \times \{0, \dots, q-2\}) \setminus \{(p-2, q-2)\}, \quad (19)$$

we have that the other critical points of type (iv) are given in the chart \tilde{X}_1 by

$$(\alpha^{n+m(q-1)} \lambda_{1,\mathrm{crit}}^+, \alpha^{n(\frac{p}{\ell}-1)+m-\frac{m(\ell-1)q}{\ell}} \mu_{1,\mathrm{crit}}^+), \quad (20)$$

where $\alpha = e^{\frac{2\pi i \ell}{pq-p-q}}$. Of course, as in the other cases, there is redundancy in considering the full set in (19), and so we restrict to $m = 0, \dots, \frac{p}{\ell}-2$ and $n = 0, \dots, q-2$, as well as $m = \frac{p}{\ell}-1$,

$$n = 0, \dots, q - 2 - \frac{q}{\ell}.$$

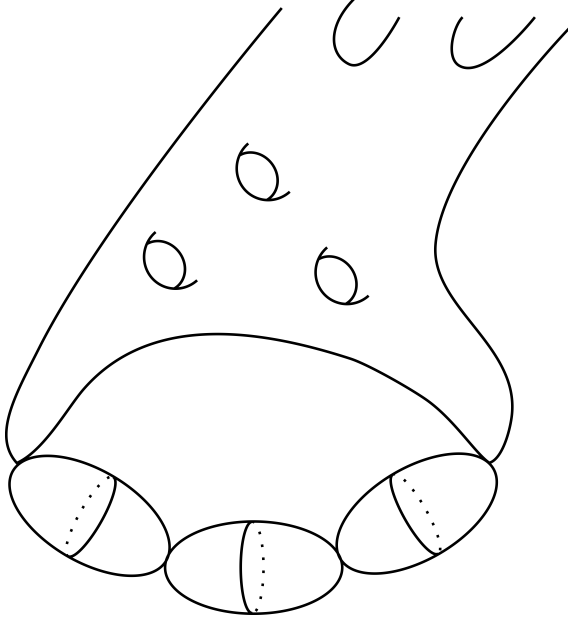


FIGURE 8. A sketch of the fibre of $\check{\mathbf{w}}_\varepsilon$ above the origin.

As computed in [Hab21, 7.1.3], the smooth fibre is a $\gcd(p, \frac{p+q}{\ell})$ -punctured curve of genus

$$g(\Sigma) = \frac{1}{2\ell}(2\ell - 1 + (p-1)(q-1) - \gcd(\ell q, p+q)).$$

We remove discs around the neck regions of Σ corresponding to the critical points whose critical value is 0, and call the resulting surface Σ' , as before. We then trivialise the fibration over a disc, identifying each fibre with Σ' . We then define the preliminary vanishing paths and cycles $V_{\lambda_i \mu_i}$ and ${}^{m,n}V_0^{\text{pr}}$ as in the loop and chain cases, taking

$$\theta_{m,n} = \frac{2\pi}{\ell} \frac{np + mq}{pq - p - q}.$$

As usual, the vanishing cycles ${}^{0,0}V_0^{\text{pr}}$ corresponds to $(\lambda_{1,\text{crit}}^+, \mu_{1,\text{crit}}^+)$, and ${}^{m,n}V_0^{\text{pr}}$ are obtained from this in Σ' by (20). The full description in Σ is given by local parallel transport considerations on the necks which were removed from Σ to give Σ' . To yield bona fide vanishing paths, we perturb the fibration slightly and introduce long fingers which go around the critical points when $\theta_{m,n} > 2\pi$ in the familiar way. As in the maximally graded case, this in fact now yields a set of transversely intersecting vanishing cycles; there is no need to isotope.

Analogously to the previous sections, we have $\arg \lambda_1 = \arg \lambda_2 = \dots = \arg \lambda_\ell$, and this argument interpolates between

$$-2\pi\ell \left(\frac{n(p-1) + m}{pq - p - q} \right) \quad \text{and} \quad 2\pi\ell \left(\frac{m(q-1) + n}{pq - p - q} \right).$$

as the modulus of λ_i increases, increasing an equal amount in each neck region. With this, it is then checked in the same way as in the previous two cases that the corresponding category $\mathcal{A}_{\check{\Gamma}}$ is presented as the quiver algebra of the quiver with relations given in Figure 7, where we use the identification

$$\begin{aligned} {}^{m,n}V_0 &\leftrightarrow {}^{i,j}K_0 & \text{with} & \quad i + m = p - 1 \\ V_{\lambda_r \mu_r} &\leftrightarrow K_{w_r}[3] & & \quad j + n = q - 1 \end{aligned} \tag{21}$$

Namely, the only compositions are the ones claimed, and the grading of the manifold is again given by the line field which is approximately horizontal on the annulus, and approximately parallel to the boundary components on connecting strips.

With all this, we arrive at the main theorem in the Brieskorn–Pham case. We state it for the non-maximally graded case, as the maximally graded case is established as a special case of [FU11].

Theorem 6.4 (Theorem 1, non-maximally graded Brieskorn–Pham polynomial case). *For a Brieskorn–Pham polynomial \mathbf{w} with grading group of index $\ell > 1$, the \mathbb{Z} -graded A_∞ -category $\mathcal{A}_{\tilde{\Gamma}}$ is described under the identification (21) by the quiver with relations in Figure 7, and is formal. In particular, by Theorem 6.1, it is quasi-equivalent to \mathcal{B} , and hence there is an induced quasi-equivalence*

$$\mathrm{mf}(\mathbb{C}^2, \Gamma, \mathbf{w}) \simeq \mathcal{FS}(\tilde{\mathbf{w}}).$$

REFERENCES

- [AR87] M. Auslander and I. Reiten. Almost split sequences for \mathbb{Z} -graded rings. *Singularities, representation of algebras, and vector bundles (Lambrecht 1985)*, 232–243, Lecture notes in Math., 1273, Springer, Berlin, 1987.
- [AKO08] D. Auroux, L. Katzarkov and D. Orlov. Mirror symmetry for weighted projective planes and their noncommutative deformations. *Ann. Math.*, Vol. 167 (2008), 867–943.
- [BH95] P. Berglund and M. Henningson. Landau–Ginzburg orbifolds, mirror symmetry and the elliptic genus. *Nucl. Phys. B*. Vol. 433 (1995), 311–332.
- [BH92] P. Berglund and T. Hübsch. A generalized construction of mirror manifolds. *Nucl. Phys. B*, Vol. 393 (1993), 377 – 391.
- [Bro88] A. Broughton. Milnor numbers and the topology of hypersurfaces. *Invent. Math.*, Vol. 92 (1988), 217–241.
- [Buc86] R-O. Buchweitz. Maximal Cohen–Macaulay modules and Tate-cohomology over Gorenstein rings. *Preprint* (1986). Available at: <https://tspace.library.utoronto.ca/handle/1807/16682>
- [BIY20] R-O. Buchweitz, O. Iyama and K. Yamura. Tilting theory for Gorenstein rings in dimension one. *Forum Math. Sigma*, Vol. 8 (2020), e37.
- [CH17] C-H. Cho and H. Hong. Finite group actions on Lagrangian Floer theory. *J. Symplectic Geom.*, Vol. 15 (2017), 307–420.
- [CCJ20] C-H Cho, D. Choa and W. Jeong. Fukaya category for Landau-Ginzburg orbifolds and Berglund-Hübsch conjecture for invertible curve singularities. *Preprint arXiv:2010.09198* (2020).
- [Dyc11] T. Dyckerhoff. Compact generators in categories of matrix factorizations. *Duke Math. J.*, Vol. 159 (2011), 223–274.
- [ET12] W. Ebeling and A. Takahashi. Mirror symmetry between orbifold curves and cusp singularities with group action. *Int. Math. Res. Not. IMRN.*, Vol. 2013 (2012), 2240–2270.
- [Eis80] D. Eisenbud. Homological algebra on a complete intersection, with an application to group representations. *Trans. Am. Math. Soc.*, Vol. 260 (1980), 35–64.
- [FJR13] H. Fan, T. Jarvis and Y. Ruan. The Witten equation, mirror symmetry, and quantum singularity theory. *Ann. Math.*, Vol. 178 (2013), 1–106.
- [FKK20] D. Favero, D. Kaplan and T. Kelly. Exceptional collections for mirrors of invertible polynomials. *Preprint arXiv: 2001.06500v2* (2020).
- [FU09] M. Futaki and K. Ueda. Homological mirror symmetry for Brieskorn–Pham singularities, *Proceedings of the 56th Japan Geometry Symposium*, 98–107, Saga University, 2009.
- [FU11] M. Futaki and K. Ueda. Homological mirror symmetry for Brieskorn–Pham singularities, *Selecta Math. (N.S.)*, Vol. 17 (2011), 435–452.
- [FU13] M. Futaki and K. Ueda. A note on homological mirror symmetry for singularities of type D. *Math. Z.*, Vol. 273 (2013), 633–652.
- [Hab21] M. Habermann. Homological mirror symmetry for nodal stacky curves *Preprint arXiv:2101.12178* (2021).
- [Hab22] M. Habermann. Homological mirror symmetry for invertible polynomials in two variables. *Quantum Top.*, Vol. 13 (2022), 207–253.
- [HS20] M. Habermann and J. Smith. Homological Berglund–Hübsch mirror symmetry for curve singularities. *J. Symp. Geom.*, Vol. 18 (2020), 1515–1574.
- [HO20] Y. Hirano and G. Ouchi. Derived factorization categories of non-Thom–Sebastiani-type sums of potentials. *Preprint arXiv:1809.09940v2* (2020).
- [IT13] O. Iyama and R. Takahashi. Tilting and cluster tilting for quotient singularities. *Math. Ann.*, Vol. 356 (2013), 1065–1105.
- [Kra10] M. Krawitz. *FJRW rings and Landau–Ginzburg mirror symmetry*. PhD Dissertation, University of Michigan, Ann Arbor (2010). Available at: <https://www.proquest.com/docview/762374402?parentSessionId=euqFJiQhhDbpX21Uun7IZFjqpZ0BS%2BEeBgrd5gaPrFw%3D>.
- [Kra19] O. Kravets. Categories of singularities of invertible polynomials. *Preprint arXiv:1911.09859* (2019).

- [KS92] M. Kreuzer and H. Skarke. On the classification of quasihomogeneous functions. *Comm. Math. Phys.*, Vol. 150 (1992), 137-147.
- [LU22] Y. Lekili and K. Ueda. Homological mirror symmetry for Milnor fibers via moduli of A_∞ -structures. *J. Topol. (To appear)*, (2022).
- [Orl09] D. Orlov. Derived categories of coherent sheaves and triangulated categories of singularities. *Algebra, arithmetic, and geometry: in honor of Yu. I. Manin. Vol. II*, Vol. 270 of Progr. Math., 503-531. Birkhäuser Boston, Inc., Boston, MA (2009).
- [Sei00] P. Seidel. Graded Lagrangian submanifolds. *Bull. Soc. Math. France*, Vol. 128 (2000), 103-149.
- [Sei08] P. Seidel. Fukaya categories and Picard-Lefschetz theory. Zurich Lectures in Advanced Mathematics. European Mathematical Society (EMS), Zürich (2008).
- [Tak10] A. Takahashi. Weighted projective lines associated to regular systems of weights of dual type. *Adv. Stud. Pure Math.*, Vol. 59 (2010), 371-388.
- [Ued06] K. Ueda. Homological mirror symmetry and simple elliptic singularities. *Preprint arXiv: math/0604361* (2006).
- [PV11] A. Polishchuk and A. Vaintrob. Matrix factorizations and singularity categories for stacks. *Ann. Inst. Fourier (Grenoble)*, Vol. 61 (2011), 2609-2642.
- [PV16] A. Polishchuk and A. Vaintrob. Matrix factorizations and cohomological field theories. *J. Reine Angew. Math.*, Vol. 714 (2016), 1-122.
- [PV21] A. Polishchuk and U. Varolgunes. On homological mirror symmetry for chain type polynomials. *Preprint arXiv: 2105.03808* (2021).
- [Rei03] M. Reid. Surface cyclic quotient singularities and HirzebruchJung resolutions. *Lecture notes* (2003). Available at: <http://homepages.warwick.ac.uk/~masda/surf/more/cyclic.pdf>.

UNIVERSITÄT HAMBURG, FACHBEREICH MATHEMATIK, BUNDESSTRASSE 55, 20146 HAMBURG, GERMANY
E-mail address: matthew.habermann@uni-hamburg.de